

# Modeling zooplankton growth in Lake Washington: A mechanistic approach to physiology in a eutrophication model



Gurbir Perhar<sup>a,\*</sup>, George B. Arhonditsis<sup>a</sup>, Michael T. Brett<sup>b</sup>

<sup>a</sup> Ecological Modeling Lab, University of Toronto, 1265 Military Trail, Scarborough, Ontario, M1C 1A4 Canada

<sup>b</sup> Department of Civil & Environmental Engineering, University of Washington, Seattle, WA 98195-2700, USA

## ARTICLE INFO

### Article history:

Received 15 October 2012

Received in revised form 19 February 2013

Accepted 22 February 2013

### Keywords:

Highly unsaturated fatty acids

Zooplankton

Growth limitation

Stoichiometry

Management-oriented models

Eutrophication

## ABSTRACT

Many efforts have been made to incorporate our improved understanding of zooplankton physiology and behaviour into mathematical models. The increased complexity, however, has been a major impediment in integrating these advances into management-oriented models and thus bridging the gap between theoretical and applied ecology. In this study, we enhance an existing eutrophication model with a zooplankton somatic growth submodel that simulates the interplay among nitrogen, phosphorus, and highly unsaturated fatty acids (HUFAs) through the grazers' digestive tracks. We calibrate the newly incorporated parameters (and associated processes) against observed data from the mesotrophic Lake Washington. We extrapolate the model to different trophic environments and tease out the underlying drivers of zooplankton growth. Our analysis suggests that both stoichiometric and HUFA based somatic growth limitations can modulate the zooplankton biomass in mesotrophic environments. Food abundance and mineral P limitation are critical factors of zooplankton growth under oligotrophic conditions, while HUFA availability is the main driving force of plankton dynamics in eutrophic states. Our zooplankton submodel downplays pre-gut regulation in favour of post-gut metabolic processing, which appears to shift the bulk of the non-limiting nutrient recycling from particulate to dissolved form. The homeostatic maintenance of somatic quotas and the dynamic nutrient recycling could also be an important mechanism for shedding light on the controversial hypothesis that the enrichment of natural ecosystems is a destabilizing factor of food web dynamics.

© 2013 Elsevier B.V. All rights reserved.

## 1. Introduction

Modeling the organized complexity of an ecosystem requires simplifications to balance ecological mechanics with available knowledge. Plankton population models can be either empirical or mechanistic, but the latter are more prevalent in theory-building studies (Mooij et al., 2010) and provide superior predictive capabilities (Baird, 1999). If the aim of a given model is to explain large scale patterns rather than describe them, the patterns need to be built from the processes (Royle and Dorazio, 2008). Trophic interactions between primary producers and grazers are arguably the most important in aquatic food webs (Brett and Müller-Navarra, 1997), but modeling a zooplankton community is intrinsically more difficult than modeling an assemblage of unicellular algal species. As such, many mechanistic improvements have been proposed to the way zooplankton are modelled. These improvements range from incorporating animal behaviour, developmental traits, and internal homeostasis into larger scale frameworks.

### 1.1. Incorporating trophic strategies in zooplankton models

There are multiple formulae used in zooplankton models to describe grazing and ingestion as a function of ambient food concentration. Characteristic examples are the Ivlev equation derived from both theoretical and empirical studies (Ivlev, 1961; Parsons et al., 1969), the Michaelis-Menten equation derived from enzyme substrate kinetics, subsequently adapted to describe dissolved substrate uptake by unicellular organisms and zooplankton feeding as a function of food concentration, and the rectilinear model used to describe filter feeding (Frost, 1972; Mullin et al., 1975). Further, experimental work done by Parsons et al. (1969) and Frost (1975) provides evidence of food concentration thresholds below which feeding activity of grazers and predators ceases or dramatically decreases.

The selection of the higher predation closure term (linear, quadratic, hyperbolic or sigmoidal) can have a strong influence on the dynamics of plankton models (Edwards and Yool, 2000). Planktivorous feeding is based on the premise of a reactive distance (i.e., minimum distance at which a predator can locate specific prey), which varies widely among fish species and diminishes rapidly with light attenuation (O'Brien et al., 1979). Experimental evidence

\* Corresponding author. Tel.: +1 416 287 7690; fax: +1 416 287 7279.  
E-mail address: [g.perhar@mail.utoronto.ca](mailto:g.perhar@mail.utoronto.ca) (G. Perhar).

suggests pursuit is based on apparent size, such that predators go after the larger, most proximal prey (O'Brien et al., 1979). Spatially explicit behavior, however, may be difficult to model as a common simplification employed in plankton models is their reduced dimensionality (e.g., zero dimensional population model approximating pelagic conditions as in Perhar and Arhonditsis, 2009).

### 1.2. Incorporating spatial behaviour into zooplankton models

Many food web models ignore individuals' processing of fitness and treat animals as particles controlled entirely by their surroundings (Fiksen and Carlotti, 1998). Aita et al. (2003) highlight the importance of zooplankton diel vertical migration (DVM) in plankton models. Fiksen and Carlotti (1998) argue that the shift from dangerous but food rich regions to cold and relatively barren regions with reduced predation is an important phenomenon. However, modeling zooplankton movement presents difficulties such as quantifying the relative importance of different selective forces. Temperature, food availability, predation risk, predator regime, and organism size at maturity are all examples of possible selective forces driving DVM (Lampert, 1989).

An additional complication in modeling zooplankton dynamics is quantifying the interactions of individual zooplankters with the environment and one another. Many zooplankton species are known to form swarms and schools, resulting in unevenly distributed zooplankton in both vertical and horizontal directions. Mathematical models for the formation and maintenance of zooplankton swarms must consider Newton's equation of motion, Stokes' law and Reynolds number to describe animal swarming motion and the associated fluid dynamics (Okubo and Anderson, 1984). Further, many factors control zooplankton swimming behaviour, e.g., species (Tiselius and Jonsson, 1990), age (Coughlin et al., 1992; vanDuren and Videler, 1995; Fisher et al., 2000; Titelman, 2001), prey density (Tiselius, 1992; Bundy et al., 1993; Dowling et al., 2001), presence of predators or a conspecific (vanDuren and Videler, 1996; Tiselius et al., 1997; Titelman, 2001), individuals' sex (vanDuren and Videler, 1995; Brewer, 1998; Strickler, 1998), and hydrodynamic effects of swimming by other animals in the area (Yen and Strickler, 1996; Gries et al., 1999). Unfortunately, there are far fewer studies analyzing movement patterns of aquatic micro organisms than their terrestrial counterparts; see Seuront et al. (2003) for a detailed mathematical description of zooplankton swimming behaviour.

Further difficulties in modeling the dynamics of zooplankton assemblages stem from the diversity of form, behaviour, and function (Bryant et al., 1997). The traditional perception of strict herbivorous feeding is now challenged as misleading, as many species can function as omnivores, which is a difficult feature to model (Lonsdale et al., 1979; Sherr et al., 1986; Conley and Turner, 1987; Kleppel et al., 1988). Zooplankton body size can vary by two orders of magnitude over the life cycle of certain species (Bryant et al., 1997). Explicit consideration of allometric scaling of physiological rates may be vital where zooplankton parameterizations are heavily dependent on animal age, developmental stage or body weight (Bryant et al., 1997). Another promising aspect towards improving the zooplankton spatial behavioural patterns could be the work done by Fennel and Neumann (2001), who model copepod life stages (eggs, nauplii, copepodites, and adults) and the associated metabolic processes (e.g., hatching and moulting) and energetic costs.

### 1.3. Incorporating intra-organism processes into zooplankton models

Another trend in the contemporary zooplankton modeling practice is to augment the representation of sub organismal

processes. For example, Sjöberg (1980) considered two zooplankton ingestion–digestion schemes: (i) grazer is assumed to search and filter at maximum rate until gut is completely filled; (ii) grazer is assumed to continuously change feeding strategy in response to gut contents. Queueing theory introduced by Sjöberg (1980) treats food particles in the gut as a queue, with digestion as a service given only to the food item holding first position, and assumes the digestive process to be the limiting factor rather than the capture and ingestion of food. A more recent series of zooplankton models investigate internal homeostasis by explicitly tracking food particles and their constituent nutrients through a grazer. Anderson et al. (2005) investigate the fate of grazed nutrients in an individual cladoceran model, built upon the framework set by Andersen (1997). Somatic processes considered include respiration, assimilation, and maintenance turnover rates. Advancements in this direction introduce the stoichiometric perspective into zooplankton feeding behaviour, and allow for a better understanding of the indirect impacts of zooplankton on phytoplankton (e.g., nutrient recycling rates; see Ramin et al., 2012).

In this study, our objective is to incorporate the proposed growth submodel into the eutrophication model originally developed for the mesotrophic Lake Washington (Arhonditsis and Brett, 2005a,b). First, we provide the rationale for the model structure adopted, the simplifications included, and the formulations used during the development phase of the model. We then present the results of a calibration exercise and examine the ability of the model to sufficiently reproduce the average observed conditions in Lake Washington along with the actual ecological processes and the cause–effect relationships in the system. The behaviour of the new zooplankton growth submodel is examined in the extrapolation domain (oligo-, eutrophic conditions), in order to gauge the impacts of the newly incorporated processes. Finally, we discuss the capacity of the new submodel to shed light on the representation of producer–grazer interactions. In particular, we focus on the impacts of pre- and post-gut somatic regulations on nutrient recycling. Specifically, we address the issue of the stoichiometric signature of the material egested by zooplankton and its fate in the system. We conclude by discussing future augmentations of the zooplankton growth submodel proposed.

## 2. Methodology

### 2.1. Host model description

The base model on which the zooplankton growth submodel is applied is the eutrophication model developed for Lake Washington (Arhonditsis and Brett, 2005a). The original model considers five nutrient cycles (organic carbon, nitrogen, phosphorus, silica, dissolved oxygen), three phytoplankton (diatoms, greens, cyanobacteria), and two zooplankton (copepods, cladocerans) functional groups. The overall topology of the system remains in tact (see Fig. 1(a)), as our restructuring only alters the two grazer compartments. An overview of the processes included in the host model is provided in the electronic supplementary material, but we refer the reader to Arhonditsis and Brett (2005a) for a detailed synopsis on Lake Washington background, bathymetry, hydrological and nutrient loading forcing.

### 2.2. Zooplankton growth submodel description

Additions to the host eutrophication model account for the post-grazing fates of ingested substrates, and their impacts on consumer growth (see Fig. 2). Perhar et al. (2012b) introduced this zooplankton growth submodel, building on the framework of Anderson et al. (2005), with explicit consideration of nutrients and HUFAs

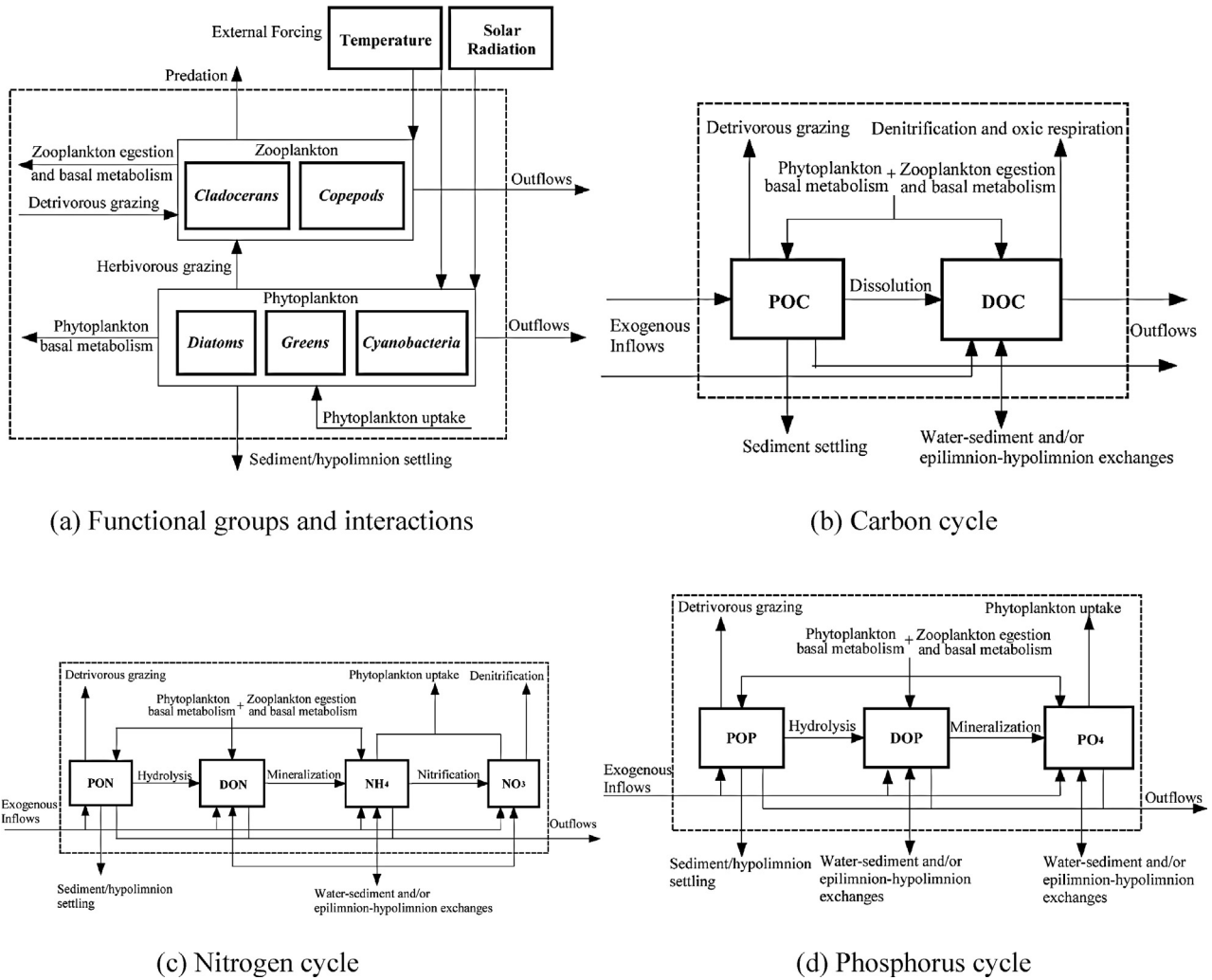


Fig. 1. (a–d) Eutrophication model for Lake Washington mass flow topology as presented in Arhonditsis and Brett (2005a).

in an individual zooplankter. Tracking growth limiting compounds through a grazers gut and dynamically modelling zooplankton growth drove macroscopic ecological patterns from microscopic physiological processes (Perhar et al., 2012c). In the present study, both cladoceran and copepod growth rates are calculated explicitly, incorporating the mechanics introduced by Perhar et al. (2012b). The growth submodel requires additional characteristics of phytoplankton and detritus in order to drive zooplankton growth. As such, eicosapentaenoic acid (EPA) and docosahexaenoic acid (DHA) concentrations of the three algal groups ( $PHYT_{i_{EPA:C}}$ ,  $PHYT_{i_{DHA:C}}$ ) and detritus ( $DET_{EPA:C}$ ,  $DET_{DHA:C}$ ) need to be specified. The nitrogen and phosphorus algal content was explicitly modelled, through the luxury uptake consideration of the original model (Arhonditsis and Brett, 2005a; Zhao et al., 2008a), whereas the corresponding levels in detritus are user specified. Seston food quality was represented by a combined food quality index, which was a surrogate of the impact of biochemical food quality, morphology, ingestibility, and toxicity (Zhao et al., 2008b). The same index in the new model reflects only the causal association between morphological properties and seston food quality. Namely, total food quality is the sum of all food sources (i.e.,  $PHYT_i$  and  $DET$ ) weighted by their respective food quality indices (i.e.,  $FQ_{PHYT_i}$  and  $FQ_{DET}$ ) reflecting the morphological features (i.e., ingestibility, digestibility, and toxicity) of the grazed seston (see Perhar et al., 2012b,c for details).

$$FQ_{TOT} = \left[ \sum_i FQ_{PHYT_i}^2 \sqrt{PHYT_i} + FQ_{DET}^2 \sqrt{DET} \right] Z_{PLIM}$$

$$i = diatoms, greens, cyanobacteria \quad (1)$$

The parameter  $Z_{PLIM}$  accounts for secondary limitation resulting from the imbalance between the  $P : C$  ratio of the grazed seston ( $GRAZ_P$ ; see Eq. (5)) and the critical minimum phosphorus somatic quota ( $P_{M_j}$ ):

$$\text{if } GRAZ_P \leq P_{M_j}, \quad Z_{PLIM_j} = \frac{GRAZ_P}{P_{M_j}}, \quad j = copepod, cladoceran$$

$$\text{if } GRAZ_P > P_{M_j}, \quad Z_{PLIM_j} = 1 \quad (2)$$

After the addition of our zooplankton growth submodel, Eq. (2) accounts for the indirect limitation imposed by P-limited algae which can undergo structural and morphological changes (thicker cell walls) that reduce their digestibility (Van Donk and Hessen, 1993; Ravet and Brett, 2006). To recap, total food quality determines the extent to which ingested food is either assimilated or egested (i.e., via sloppy feeding) based on morphological characteristics.

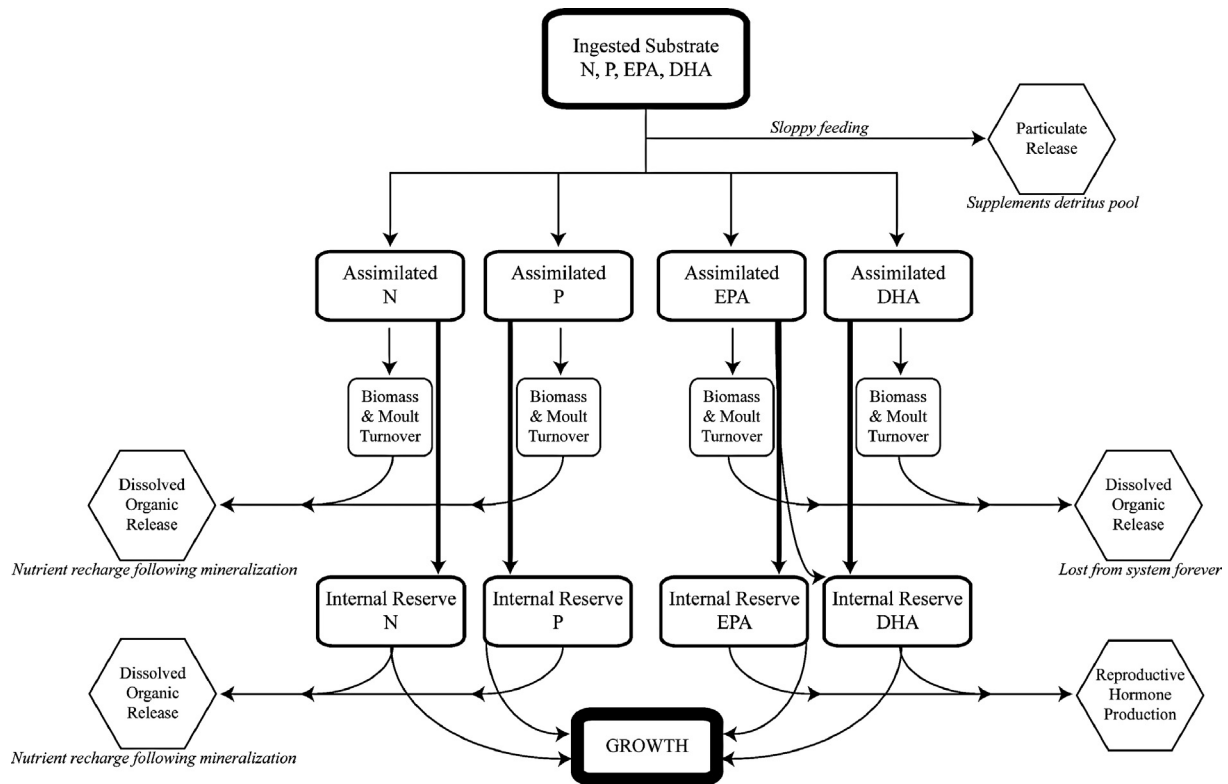


**Fig. 2.** Grazer HUFA sub model. Ingested matter is assimilated or egested via sloppy feeding based on morphological properties. Assimilated substrates are subject to maintenance costs (i.e., moults and biomass turnover). Remaining substrates are added to the internal quotas, which are regulated by nutrient release and taxed for hormonal production, before fueling growth. Dissolved nutrient release is subject to mineralization, whereas dissolved HUFA release is assumed to be lost to the system.

Respiration costs of assimilation are implicitly considered ( $\alpha_{C1}$  and  $\alpha_{C2}$ ) in the calculation of carbon assimilation efficiency ( $\alpha_C$ ):

$$\alpha_{Cj} = \frac{\alpha_{C1j} FQ_{TOT}}{\alpha_{C2j} + FQ_{TOT}} \quad (3)$$

To calculate the carbon assimilation rate ( $\alpha_{SC}$ ), carbon assimilation efficiency is multiplied by grazed particulate carbon rate, which in turn is modelled as a function of zooplankton maximum grazing rate ( $\lambda$ ), zooplankton grazing preference for the different phytoplankton groups ( $\omega_{PHYT}$ ) and detritus ( $\omega_{DET}$ ), available phytoplankton and detritus biomass, and zooplankton grazing half saturation constant ( $\mu$ ):

$$\alpha_{SCj} = \frac{\lambda_j \alpha_{Cj} (\sum_i \omega_{PHYT_{ij}} PHYT_i^2 + \omega_{DETj} DET_C^2)}{\mu_j^2 + \sum_i \omega_{PHYT_{ij}} PHYT_i^2 + \omega_{DETj} DET_C^2} \quad (4)$$

The resource concentrations in algae and detritus (phosphorus:  $PC_i$  and  $DET_{P:C}$ ; nitrogen:  $NC_i$  and  $DET_{N:C}$ ; EPA:  $PHYT_{iEPA:C}$  and  $DET_{EPA:C}$ ; DHA:  $PHYT_{iDHA:C}$  and  $DET_{DHA:C}$ ) are parameterized, allowing for the separation of grazed food per unit of biomass into four separate pools, i.e., phosphorus, nitrogen, EPA and DHA; Eqs. (5)–(8), respectively:

$$GRAZ_{Pj} = \frac{\sum_i \omega_{PHYT_{ij}} PHYT_i^2 PC_{PHYT_i} + \omega_{DETj} DET_C^2 DET_{P:C}}{\sum_i \omega_{PHYT_{ij}} PHYT_i^2 + \omega_{DETj} DET_C^2} \quad (5)$$

$$GRAZ_{Nj} = \frac{\sum_i \omega_{PHYT_{ij}} PHYT_i^2 NC_{PHYT_i} + \omega_{DETj} DET_C^2 DET_{N:C}}{\sum_i \omega_{PHYT_{ij}} PHYT_i^2 + \omega_{DETj} DET_C^2} \quad (6)$$

$$GRAZ_{EPAj} = \frac{\sum_i \omega_{PHYT_{ij}} PHYT_i^2 PHYT_{iEPA:C} + \omega_{DETj} DET_C^2 DET_{EPA:C}}{\sum_i \omega_{PHYT_{ij}} PHYT_i^2 + \omega_{DETj} DET_C^2} \quad (7)$$

$$GRAZ_{DHAj} = \frac{\sum_i \omega_{PHYT_{ij}} PHYT_i^2 PHYT_{iDHA:C} + \omega_{DETj} DET_C^2 DET_{DHA:C}}{\sum_i \omega_{PHYT_{ij}} PHYT_i^2 + \omega_{DETj} DET_C^2} \quad (8)$$

Assimilated substrate rate is calculated by multiplying grazed substrate per unit of biomass with the carbon assimilation rate (see Eqs. (9)–(12)). Thus, the assimilation of a particular substrate depends only on the morphological characteristics and substrate ratios of the grazed seston.

The first physiological need addressed by the ingested material is maintenance in the forms of biomass and moults turnover rates, i.e.,  $T_{resource}$  and  $T_m$ , respectively. Consequently, post-maintenance resource pools ( $resource_{PM}$ ; Eqs. (9)–(12)) reflect the difference between assimilated substrates, and substrates removed in somatic maintenance:

$$P_{PMj} = \alpha_{SCj} GRAZ_{Pj} - P_{INTj} (T_{Pj} (1 - m_j) - m_j T_{mj}) \quad (9)$$

$$N_{PMj} = \alpha_{SCj} GRAZ_{Nj} - N_{INTj} (T_{Nj} (1 - m_j) - m_j T_{mj}) \quad (10)$$

$$EPA_{PMj} = (1 - \epsilon_j) [\alpha_{SCj} GRAZ_{EPAj} - EPA_{INTj} (T_{EPAj} (1 - m_j) - m_j T_{mj})] + v_j \sum_i \eta_{PUFAi} \quad (11)$$

$$DHA_{PMj} = \alpha_{SCj} GRAZ_{DHAj} - DHA_{INTj} (T_{DHAj} (1 - m_j) - m_j T_{mj}) + \rho_j \epsilon_j EPA_{PMj} \quad (12)$$

In Eqs. (11) and (12), we assume a fraction of the post-maintenance EPA pool is subject to elongation to DHA (see Persson and Vrede, 2006; Perhar et al., 2012b), parameterized by the EPA fraction allocated to elongation ( $\epsilon_1$ ) and the elongation efficiency ( $\rho$ ). We also note that our model does not consider retro-conversion of DHA to EPA. Elongation of polyunsaturated fatty acids (PUFAs)

**Table 1**  
Description and calibration values of zooplankton submodel parameters.

Parameter	Symbol	Unit	Copepod	Cladoceran
Somatic P turnover rate	$T_{Pj}$	day <sup>-1</sup>	0.025	0.025
Somatic N turnover rate	$T_{Nj}$	day <sup>-1</sup>	0.025	0.025
Somatic EPA turnover rate	$T_{EPAj}$	day <sup>-1</sup>	0.005	0.005
Somatic DHA turnover rate	$T_{DHAj}$	day <sup>-1</sup>	0.005	0.005
Somatic moult turnover rate	$T_{Mj}$	day <sup>-1</sup>	0.05	0.05
Somatic moult fraction	$m_j$	unitless	0.05	0.05
EPA to DHA fraction	$\epsilon_j$	unitless	0.25	0.05
EPA to DHA efficiency	$\rho_j$	mg DHA (mg EPA) <sup>-1</sup>	0.5	0.05
PUFA to EPA efficiency	$\nu_j$	mg EPA (mg PUFA) <sup>-1</sup>	0.025	0.025
Somatic P excretion rate	$\chi_{Pj}$	day <sup>-1</sup>	0.002	0.002
Somatic N excretion rate	$\chi_{Nj}$	day <sup>-1</sup>	0.002	0.002
EPA hormone production rate	$h_{EPAj}$	day <sup>-1</sup>	0.015	0.015
DHA hormone production rate	$h_{DHAj}$	day <sup>-1</sup>	0.015	0.025
Minimum somatic P	$P_{Mj}$	mg P (mg C) <sup>-1</sup>	0.0002	0.002
Optimum somatic P	$P_{Oj}$	mg P (mg C) <sup>-1</sup>	0.015	0.025
Minimum somatic N	$N_{Mj}$	mg N (mg C) <sup>-1</sup>	0.09	0.05
Optimum somatic N	$N_{Oj}$	mg N (mg C) <sup>-1</sup>	0.15	0.105
Minimum somatic EPA	$EPA_{Mj}$	mg EPA (mg C) <sup>-1</sup>	0.001	0.005
Optimum somatic EPA	$EPA_{Oj}$	mg EPA (mg C) <sup>-1</sup>	0.009	0.012
Minimum somatic DHA	$DHA_{Mj}$	mg DHA (mg C) <sup>-1</sup>	0.004	0.0009
Optimum somatic DHA	$DHA_{Oj}$	mg DHA (mg C) <sup>-1</sup>	0.012	0.005
Maximum somatic growth rate	$\pi_{MAXj}$	day <sup>-1</sup>	0.33	0.68

to EPA are determined by the PUFA flux from grazed seston ( $\eta_{PUFA_i}$ ) and somatic elongation efficiency ( $\rho$ ). Elongation is an inefficient process, and the calibration vector presented herein (see Table 1) postulates that copepods are more likely to elongate EPA to DHA than cladocerans (Ravet et al., 2010). The zooplankton growth submodel affords zooplankters the ability to shut certain processes down if homeostasis is at risk. If for example, the internal EPA falls below 50% saturation, elongation of EPA to DHA and other EPA expenditures cease; if internal DHA saturation falls below 50%, DHA contribution to reproduction also ceases (see Perhar et al., 2012c).

Finally, there are post-maintenance costs to consider for each resource pool before somatic growth ( $\pi_j$ ) and internal resource concentrations are calculated. The nitrogen and phosphorus pools are subjected to a regulated release fraction ( $\chi$ ). Conceptually, these releases represent post-gut excretion in the forms of urine and feces, but can also be thought of as a homeostatic regulation mechanism. Aggressive accrual is addressed using a second excretion mode: *venting* (as opposed to *regular*). Regular mode refers to the excretion rate prespecified in the calibration vector, while *venting* mode refers to an accelerated release. For simplicity sake, regulatory excretion is limited to regular mode until internal resource storage surpasses the optimal threshold, at which point excretion is set to *venting* mode at a value of 0.1 (see Fig. 1a in ESM). Once accounted for, the somatic nutrient concentration differential equations can be calculated as:

$$\frac{dP_{INTj}}{dt} = P_{PMj} - P_{INTj}(\pi_j + \chi_{Pj}) \quad (13)$$

$$\frac{dN_{INTj}}{dt} = N_{PMj} - N_{INTj}(\pi_j + \chi_{Nj}) \quad (14)$$

Pre-gut regulation releases substrate into the water column in particulate form (via sloppy feeding), but maintenance byproducts and post-maintenance release can be fractionated into ammonium, dissolved organic nitrogen, dissolved organic phosphorus, and phosphate. The rate of change of somatic HUFAs concentrations are specified as follows:

$$\frac{dEPA_{INTj}}{dt} = EPA_{PMj} - EPA_{INTj}(\pi_j + h_{EPAj}) \quad (15)$$

$$\frac{dDHA_{INTj}}{dt} = DHA_{PMj} - DHA_{INTj}(\pi_j + h_{DHAj}) \quad (16)$$

where  $h$  is the fraction of HUFAs allocated for hormone production.

Somatic resource saturation quotients ( $g_{LIM_{resourcej}}$ ) are calculated as follows:

$$g_{LIMPj} = \frac{P_{INTj} - P_{Mj}}{P_{Oj} - P_{Mj}} \quad (17)$$

$$g_{LIMNj} = \frac{N_{INTj} - N_{Mj}}{N_{Oj} - N_{Mj}} \quad (18)$$

$$g_{LIMEPAj} = \frac{EPA_{INTj} - EPA_{Mj}}{EPA_{Oj} - EPA_{Mj}} \quad (19)$$

$$g_{LIMDHAj} = \frac{DHA_{INTj} - DHA_{Mj}}{DHA_{Oj} - DHA_{Mj}} \quad (20)$$

where  $Resource_{Mj}$  and  $Resource_{Oj}$  represent the minimum and optimum somatic requirements respectively, of a zooplankter for the different nutritional factors considered.

Finally, the resource saturation equations are used to quantify zooplankton growth using an approach that resembles *Liebig's Law of the Minimum*, postulating the grazer's growth is limited by the resource in shortest supply with no regard for whether limitation stems from mineral or HUFAs deficiency:

$$\pi_j = \pi_{MAXj} \min[g_{LIMPj}, g_{LIMNj}, g_{LIMEPAj}, g_{LIMDHAj}] \quad (21)$$

where  $\pi_{MAXj}$  is the maximum somatic growth rate when prevailing ambient conditions are optimal.

### 2.3. Procedure

Integration of the zooplankton growth submodel into the host model consisted of substituting cladoceran and copepod growth rates in both the epilimnion and hypolimnion with those calculated by the submodel. Additional parameters were added to the host model to account for diatom, green algae, cyanobacteria, and particulate organic carbon (detritus) EPA:C and DHA:C fractions. The nominal food qualities for each of the aforementioned food sources were updated to reflect the changes outlined previously (nominal food quality now represents morphology and not nutritional value). Finally, the only other change to the host model's parameterization was the adjustment of the ammonium inhibition for nitrate uptake ( $\psi$ ) value to improve the fit of ammonium to the observed data

**Table 2**  
Description and calibration values of seston model parameters.

Parameter	Symbol	Unit	Diatom	Green	Cyanobacteria	Detritus
Seston EPA:C ratio	$PHYT_i, DET_{EPA:C}$	mg EPA (mg C) <sup>-1</sup>	0.035	0.0001	0.0001	0.001
Seston DHA:C ratio	$PHYT_i, DET_{DHA:C}$	mg DHA (mg C) <sup>-1</sup>	0.02	0	0.0001	0.001
Seston PUFA:C ratio	$\eta_{PUFAi}$	mg PUFA (mg C) <sup>-1</sup>	0.008	0.06	0.015	0.001
Seston morphology	$FQ_{PHYT_i, DET}$	unitless	0.9	0.5	0.35	0.5

(see Arhonditsis and Brett, 2005b). Additionally, zooplankton nutrient turnover rates were assumed to be in dissolved organic form, and were added to the recycling loops in their respective nutrient cycles.

The parameters associated with the explicit zooplankton growth submodel were calibrated against observed Lake Washington data reported in Arhonditsis and Brett (2005a). We also conducted a local sensitivity analysis by introducing  $\pm 15\%$  perturbations of the calibration vector. During this exercise, we also perturbed nitrogen and phosphorus loading, diffusivity, epilimnetic and hypolimnetic temperature by  $\pm 15\%$ . Two-thousand (2000) Monte Carlo simulations were used to sample the parameter space, running the model for 10 years, extracting the final annual cycle for analysis. Following the procedure in Arhonditsis and Brett (2005a), multiple linear regression analysis was carried out for epilimnetic zooplankton (cladocerans and copepods) and phytoplankton (diatoms, greens, and cyanobacteria) biomass. The entire procedure was repeated for severely reduced phosphorus loading (65% reduction of the current loading for oligotrophic conditions) and increased phosphorus loading (180% of the current loading for eutrophic conditions); these values were chosen to stretch the model, while minimizing the loss of numerical stability.

### 3. Results and discussion

#### 3.1. Model calibration

Similar to the Arhonditsis and Brett (2005b) calibration procedure, the parameterization of the model aimed to reproduce the average seasonal patterns in Lake Washington. The calibration dataset was carried over from the original study, utilizing information collected on a bi-weekly (during the summer) and monthly (the rest of the year) basis from 12 inshore and offshore sampling stations during a 7-year period (January 1995–December 2001). The calibration exercise involved tuning the submodel parameters within their reported literature ranges (see Appendix in Perhar et al., 2012b). Model performance was assessed against the average seasonal epilimnetic and hypolimnetic patterns for chlorophyll-a, phosphate, total phosphorus, nitrate, ammonium, total nitrogen, dissolved oxygen, total organic carbon, and zooplankton biomass. Our calibration vector (i.e., the parameter values providing the best fit between modelled and observed data) is reported in Tables 1 and 2. Simulated patterns are depicted against observed values for the Lake Washington epilimnion (Fig. 3) and hypolimnion (Fig. 4).

Simulated nitrate (Fig. 3c) and total nitrogen concentrations (Fig. 3b) match fairly well the observed epilimnetic data, although the latter variable seems to be more distinctly overestimated in the second half of the year. The performance of the model in regards to ammonium concentrations was significantly improved relative to the original model (see Fig. 1 in Arhonditsis and Brett, 2005b), but the model still underestimates the observed values during the spring-early summer period (Fig. 3d).

The performance of phosphate (Fig. 3e) and total phosphorus (Fig. 3f) share qualitative similarities with the original model,

such that both versions underestimate somewhat the winter levels, but fit very well the rest of the annual cycle. The model overestimates total organic carbon in the early spring, and slightly underestimates the corresponding fall values (see Fig. 3h). Predicted and observed chlorophyll-a and zooplankton biomass are in close agreement throughout the annual cycle (see Fig. 3g and i). Finally, model fit for dissolved oxygen and silica indicate no substantial change relative to the original eutrophication model (Fig. 3a and j). Compared with the Arhonditsis and Brett (2005b) study, the agreement between simulated and observed hypolimnetic dissolved oxygen and ammonium has significantly improved (Fig. 4a and d), although there is a misrepresentation of the trends in the first half of the year for ammonium. Simulated phosphate in the hypolimnion is also a marked improvement, although the new version is still subject to a higher accumulation during the summer stratified period (Fig. 4e). Total phosphorus (Fig. 4f), total organic carbon (Fig. 4h), and chlorophyll-a (Fig. 4g) in the hypolimnion are all on par with the performance of the original model throughout the annual cycle. The largest discrepancy is found with the total nitrogen levels, which are somewhat overestimated relative to the observed hypolimnetic patterns (Fig. 4b). Further, our model underestimates spring hypolimnetic nitrate, but the model fit improves significantly for the rest of the annual cycle (Fig. 4c).

We also present an assessment of the goodness-of-fit between simulated and observed monthly values for Lake Washington (see Table 3). The three diagnostic measures for this quantification were: the mean error, the relative error and the coefficient of determination. The mean error (ME) is calculated as  $\sum(\text{observed value} - \text{simulated value})/\text{number of observations}$ , and is a measure of model bias which should be close to

**Table 3**

Goodness of fit statistics for the zooplankton growth submodel, based on data presented in Arhonditsis and Brett (2005b) for total nitrogen (TN), nitrate (NO<sub>3</sub>), ammonium (NH<sub>4</sub>), phosphate (PO<sub>4</sub>), total phosphorus (TP), chlorophyll-a (Chla), total organic carbon (TOC), total zooplankton biomass (Zoop) and total epilimnetic silica (Si).

	Mean error	Relative error	r <sup>2</sup>
<b>Epilimnion</b>			
DO	0.093	0.045	0.795
TN	-23.074	0.080	0.914
NO <sub>3</sub>	31.476	0.224	0.875
NH <sub>4</sub>	7.724	0.341	0.004
PO <sub>4</sub>	0.541	0.251	0.719
TP	-3.202	0.238	0.873
Chla	-0.893	0.297	0.872
TOC	-0.107	0.156	0.002
Zoop	29.919	0.360	0.846
Si	0.098	0.268	0.623
<b>Hypolimnion</b>			
DO	0.179	0.058	0.876
TN	-60.850	0.152	0.636
NO <sub>3</sub>	56.014	0.212	0.296
NH <sub>4</sub>	4.951	0.278	0.021
PO <sub>4</sub>	-1.380	0.232	0.265
TP	-1.284	0.122	0.197
Chla	-0.699	0.471	0.753
TOC	-0.254	0.180	0.006

zero (Power, 1993). The relative error (RE) characterizes model accuracy and is calculated as  $\sum |observed\ value - simulated\ value| / \sum observed\ value$ . The coefficient of determination ( $r^2$ ) is a statistical measure commonly used in model evaluation (Mayer and Butler, 1993). Generally, the upgraded version of the model performs better in the epilimnetic compartment, when considering the RE and  $r^2$  metrics for dissolved oxygen (RE = 4.5%,  $r^2 = 0.795$ ), phosphate (RE = 25%,  $r^2 = 0.719$ ), total nitrogen ( $r^2 = 0.914$ ), total phosphorus ( $r^2 = 0.873$ ), and silica ( $r^2 = 0.623$ ). Our model fit to ammonium data was also improved on the basis of the ME value (RE = 34.1%, ME =  $7.72\ \mu\text{g L}^{-1}$ ). Our simulated hypolimnetic patterns were characterized by improved

RE and ME values for nitrate (RE = 21.2%, ME =  $56.01\ \mu\text{g L}^{-1}$ ), ammonium (RE = 27.8%, ME =  $4.95\ \mu\text{g L}^{-1}$ ), phosphate (RE = 23.2%, ME =  $-1.38\ \mu\text{g L}^{-1}$ ), and total phosphorus (RE = 12.2%, ME =  $-1.28\ \mu\text{g L}^{-1}$ ). Hypolimnetic dissolved oxygen  $r^2$  also improves relative to the original model (RE = 5.8%,  $r^2 = 0.876$ ).

Two additional scenarios were explored reproducing oligotrophic and eutrophic conditions alongside the reference mesotrophic scenario. Compared to the mesotrophic environment, where the algal composition predominantly consists of diatoms with moderate green algae and minimal cyanobacteria presence (Fig. 5c), oligotrophic conditions yield a diatom-dominated system with traces of green algae and virtually no cyanobacteria (Fig. 5a).

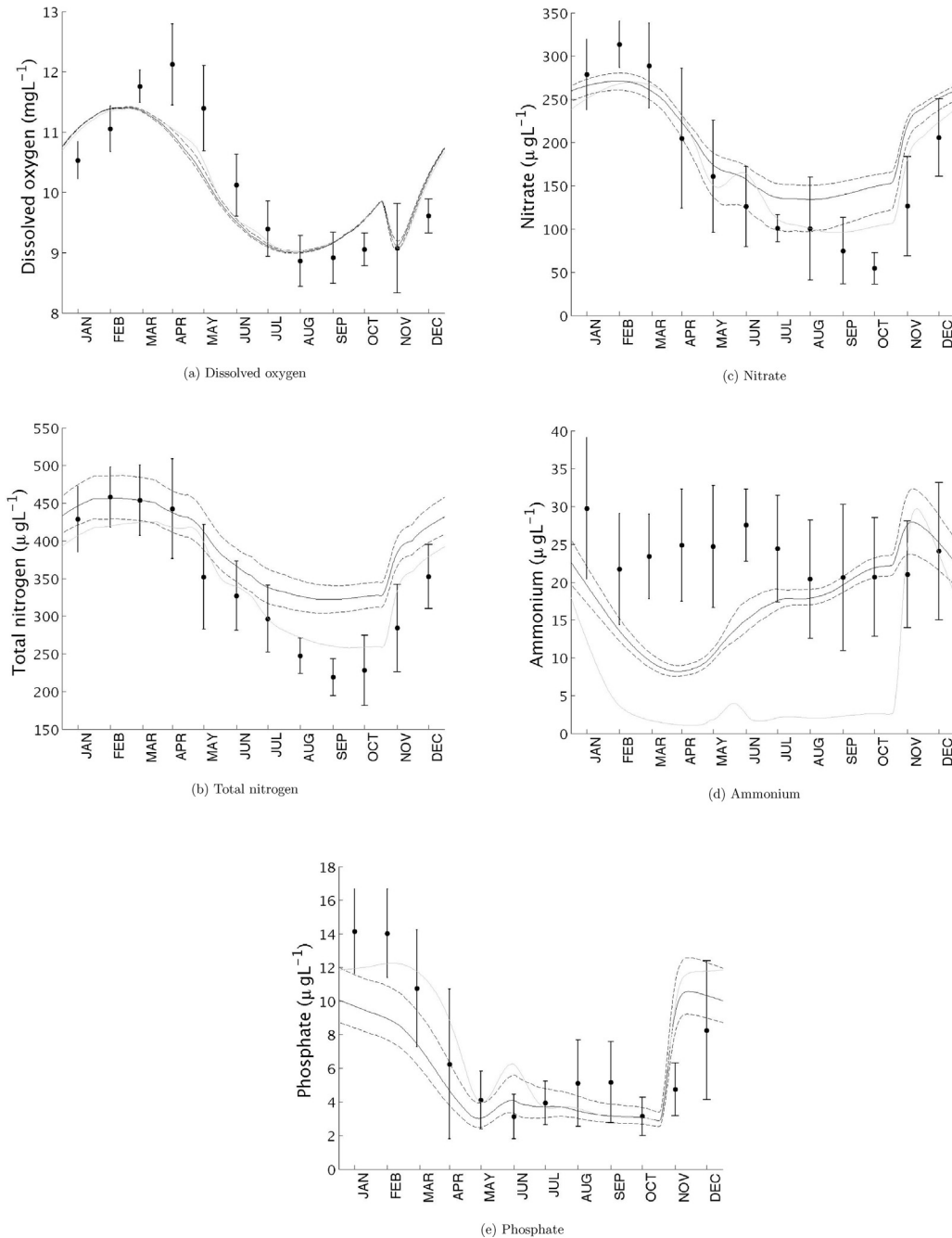


**Fig. 3.** (a–h) Epilimnetic calibration plots depicting 5th, 50th, and 95th percentiles from sensitivity analysis, against mean volume weighted variable averages (error bars represent the standard deviations for the monthly variable values for all stations and years (1995–2001) in the King County monitoring program). Calibration from original Arhonditsis and Brett (2005b) study shown in grey.

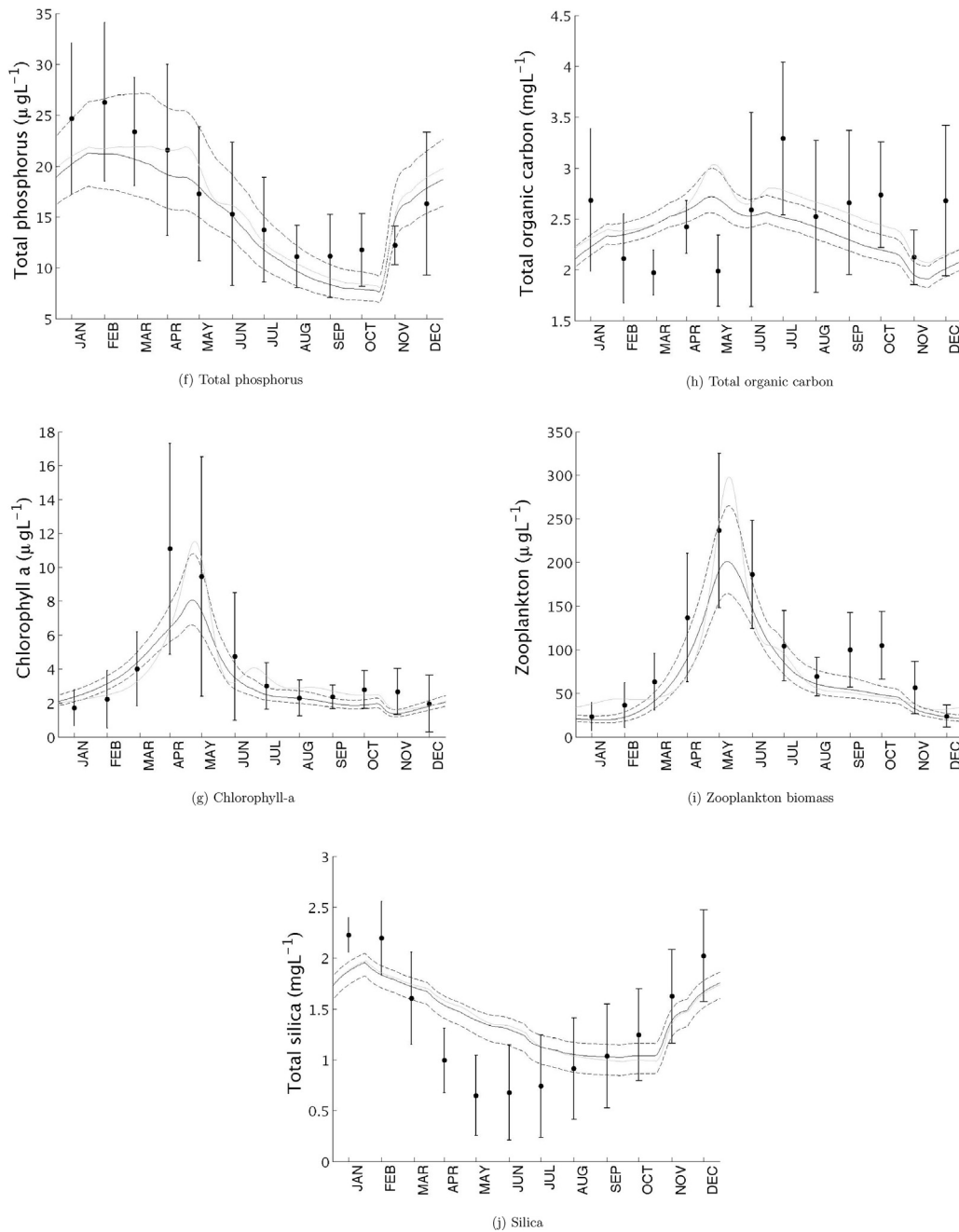


**Fig. 3.** (Continued).

However, despite the high proportion of good food quality diatoms in the algal assemblage, grazer biomass is significantly reduced due to the relatively low seston abundance in the oligotrophic environment (Fig. 5b). Phytoplankton composition was fairly even under eutrophic conditions, consisting of over 40% cyanobacteria (Fig. 5e). Yet, despite nearly double algal standing stock, total zooplankton biomass is slightly lower than in the mesotrophic setting (Fig. 5e), suggesting greater susceptibility to poor food quality conditions.

In addition to reporting model performance and plankton biomass seasonality patterns, we also highlight the factors determining somatic growth for cladocerans and copepods in different trophic states (see Fig. 6). Cladoceran somatic growth is predominantly limited by P throughout the annual cycle in our simulated oligotrophic environment. Our mesotrophic scenario shows that

mineral P limitation is most pronounced during the spring bloom and the end of summer, while cladoceran variability is modulated by seston EPA content for all the remaining months (see Fig. 6c). Under eutrophic conditions, cladoceran growth is limited by EPA throughout the year (see Fig. 6e). Notably, while our mathematical representation of somatic growth limitation allows for the consideration of multiple nutritional factors, animal biomass is ultimately modulated by the most limiting one (see Eq. (21)). However, P-limited growth in the mesotrophic spring bloom does not necessarily imply that cladocerans are starved for P, but rather that P is the least-saturated somatic resource pool and as such it drives somatic growth. We stress that starvation conditions are only exhibited once the saturation level of a resource falls below the corresponding minimum threshold (i.e.,  $R_{INT} \leq R_{MIN}$ , where  $R$

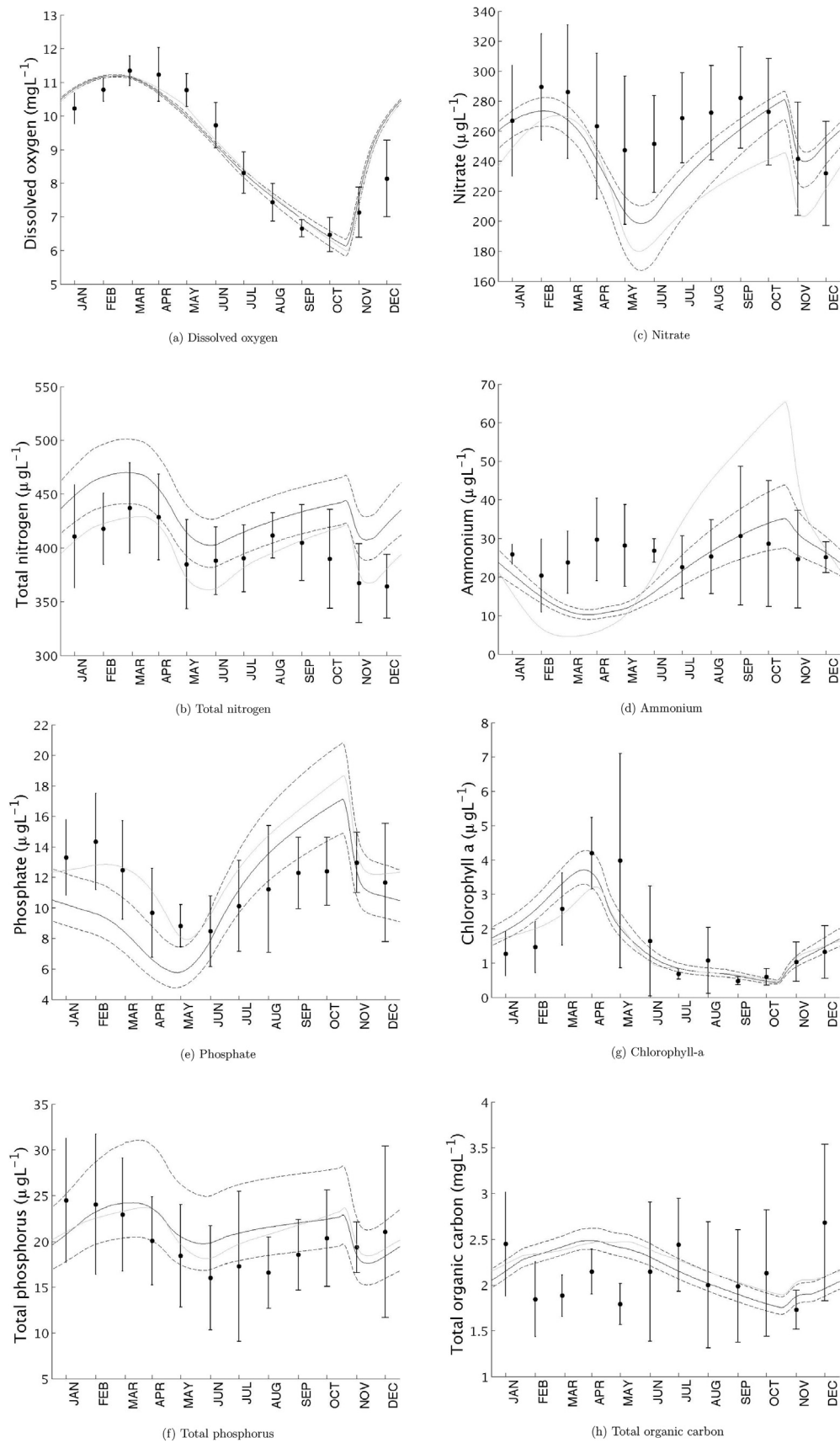


**Fig. 4.** (a–h) Hypolimnetic calibration plots depicting 5th, 50th, and 95th percentiles from sensitivity analysis, against mean volume weighted variable averages (error bars represent the standard deviations for the monthly variable values for all stations and years (1995–2001) in the King County monitoring program). Calibration from original Arhonditsis and Brett (2005b) study shown in grey.

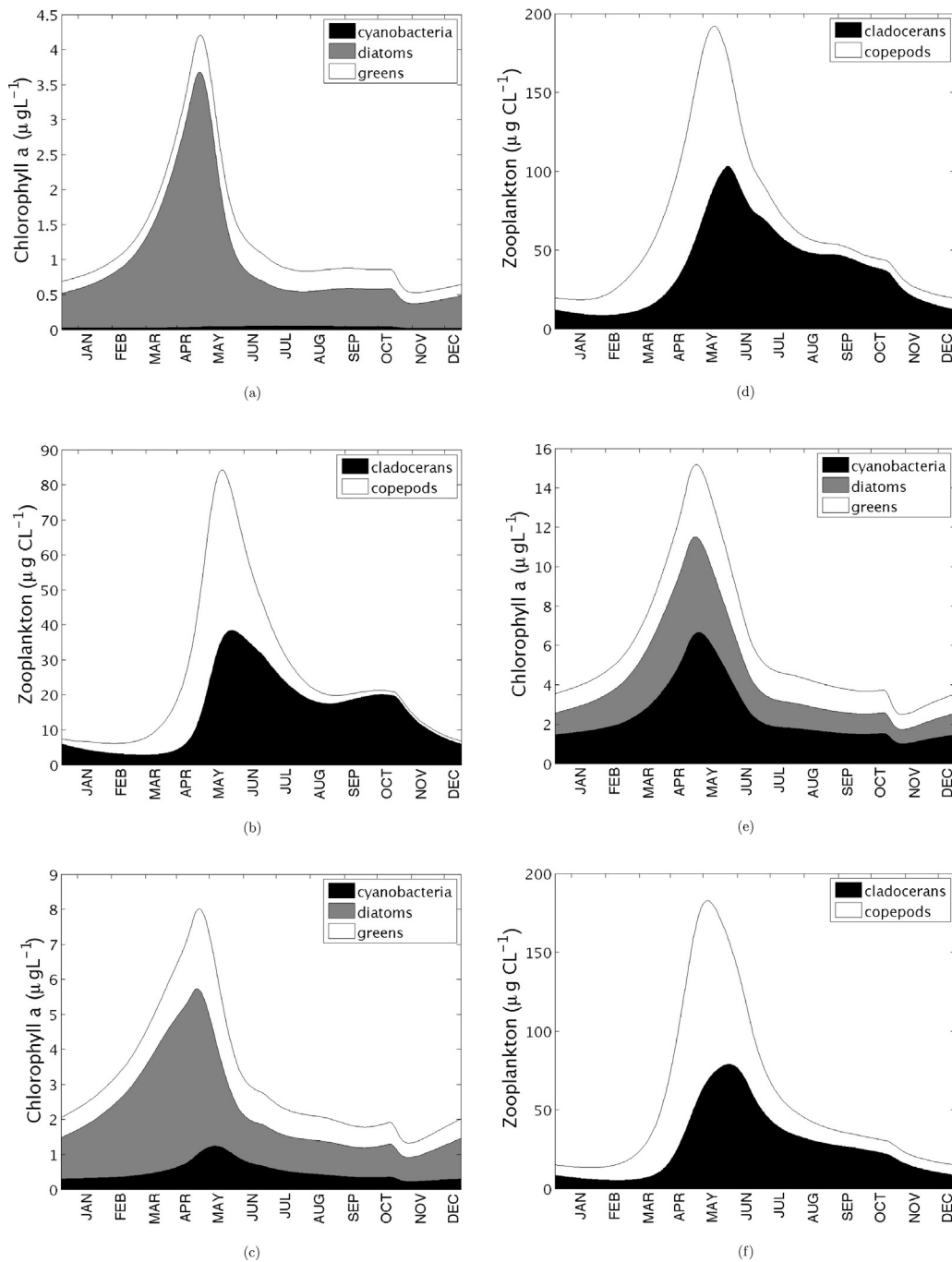


**Fig. 5.** Seasonal phytoplankton (a, c, e) and zooplankton (b, d, f) succession patterns as simulated by the zooplankton growth submodel under oligotrophic (a and b), mesotrophic (c and d), and eutrophic (e and f) conditions.

is a resource). Our framework ensures that an individual experiencing starvation, after metabolic processes are addressed, cannot grow. In addition, food availability (indicated by grazer carbon assimilation) is another important driver of zooplankton abundance (see Fig. 6a and b) but becomes less of an issue as food quantity increases (see Fig. 6e and f). Copepods experience similar limitations across the different trophic scenarios considered, but are also characterized by an interplay between N and DHA rather than P and EPA (see Fig. 6b, d, f). Finally, we note that the literature shows HUFAs comprise approximately 10% of total lipid biomass in *Daphnia* spp. collected from Lake Washington (Ravet et al., 2010). Assuming that zooplankton lipids account for 5–25% dry weight biomass (Wainman et al., 1993), and fatty acids account

for 10–73% of zooplankton lipids (Falk-Petersen et al., 1987), we approximate cladoceran HUFA:C to range from 0.00095 to 0.0493. In addition, Smyntek et al. (2008) approximates *Daphnia* total fatty acids to be  $232 \pm 56 \mu\text{g FA (mg C)}^{-1}$ , providing a HUFA:C range of 0.0134–0.0311. Our model parameterization postulates the HUFA somatic content of cladocerans to fall within the first range, and border the latter (see Fig. 7).

### 3.2. Sensitivity analysis

Multiple regression models were constructed to determine the relative impact of the zooplankton growth submodel parameters. Models were created for each month to identify seasonal influence

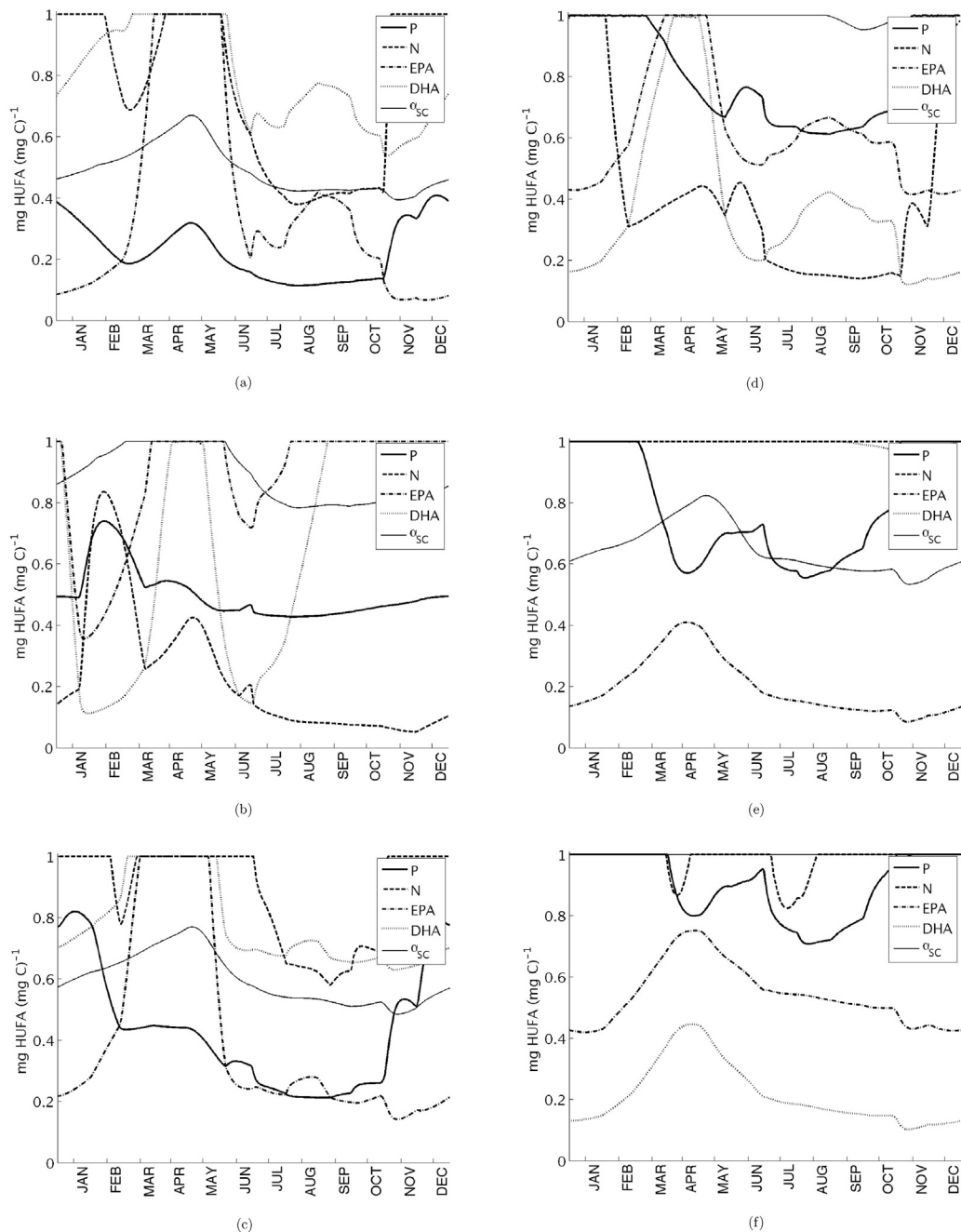


**Fig. 6.** Seasonal zooplankton growth limitation and carbon assimilation patterns across oligotrophic (a and b), mesotrophic (c and d), and eutrophic (e and f) conditions for cladocerans (a, c, e), and copepods (b, d, f).

of parameters on cladocerans, copepods, diatoms, green algae and cyanobacteria across all three trophic scenarios. The top five standardized  $\beta$  coefficients and their respective signs are reported in Tables 4 and 5.

**Cladocerans.** Multiple regression on cladoceran biomass reveals exogenous nutrient loading variability ( $W_{loading}$ ) and maximum cladoceran growth rate ( $\pi_{MAXclad}$ ) to be the two most influential parameters across all months (see Table 4). The positive sign of both parameters presumably reflects the nature of their causal link with seston abundance. Our results highlight the strong reliance of cladocerans upon the EPA availability of the grazed seston ( $DI_{EPA:C}$  and  $GR_{EPA:C}$ ). Of equal importance is their minimum EPA requirement ( $EPA_{Mclad}$ ) for maintaining their growth and normal metabolic activity. The negative nature of this causal relationship suggests that lower somatic EPA requirements render competitive

advantage and ultimately yield higher cladoceran biomass. Surprisingly, optimal somatic EPA ( $EPA_{Oclad}$ ) was never identified as a significant covariate of cladoceran growth. Optimal somatic P ( $P_{Oclad}$ ), however, had a negative relationship with cladoceran biomass throughout the growing season (from early spring to early autumn). Finally, our analysis provides evidence of competitive interactions with the other resident of our simulated zooplankton community, in that several nutritional copepod requirements ( $DHA_{Mcope}$ ,  $DHA_{Ocope}$ , and  $P_{Ocope}$ ) appear to shape the seasonal cladoceran patterns.

**Copepods.** Multiple regression results from copepod biomass under mesotrophic conditions reveal parallels with the inference drawn from cladocerans (see Table 5), i.e., the positive influence of nutrient loading ( $W_{loading}$ ) and maximum somatic growth rate ( $\pi_{MAXcope}$ ) throughout the year, and the tight link between DHA

**Table 4**  
Multiple regression analysis of the most influential model parameters for cladoceran biomass listed by month across oligotrophic, mesotrophic, and eutrophic conditions.

Oligotrophic					
JAN	FEB	MAR	APR	MAY	JUN
(+)W <sub>loading</sub>	(+)W <sub>loading</sub>	(+)W <sub>loading</sub>	(+)W <sub>loading</sub>	(-)P <sub>Oclad</sub>	(-)P <sub>Oclad</sub>
(-)EPA <sub>Mclad</sub>	(-)EPA <sub>Mclad</sub>	(+)π <sub>MAXclad</sub>	(-)P <sub>Oclad</sub>	(+)π <sub>MAXclad</sub>	(+)π <sub>MAXclad</sub>
(+)DI <sub>EPA:C</sub>	(+)DI <sub>EPA:C</sub>	(-)EPA <sub>Mclad</sub>	(+)π <sub>MAXclad</sub>	(+)W <sub>loading</sub>	(+)N <sub>Mcope</sub>
(+)π <sub>MAXclad</sub>	(+)π <sub>MAXclad</sub>	(+)P <sub>Mclad</sub>	(-)EPA <sub>Mclad</sub>	(+)W <sub>YPotemp</sub>	(+)W <sub>YPotemp</sub>
(-)CB <sub>EPA:C</sub>	(+)P <sub>Mclad</sub>	(-)P <sub>Oclad</sub>	(+)P <sub>Mclad</sub>	(-)π <sub>MAXcope</sub>	(-)T <sub>Mclad</sub>
JUL	AUG	SEP	OCT	NOV	DEC
(+)W <sub>loading</sub>	(+)W <sub>loading</sub>	(-)W <sub>loading</sub>	(+)W <sub>loading</sub>	(+)DI <sub>EPA:C</sub>	(+)W <sub>loading</sub>
(-)P <sub>Oclad</sub>	(-)P <sub>Oclad</sub>	(-)P <sub>Oclad</sub>	(-)EPA <sub>Mclad</sub>	(-)EPA <sub>Mclad</sub>	(-)EPA <sub>Mclad</sub>
(+)π <sub>MAXclad</sub>	(+)π <sub>MAXclad</sub>	(+)π <sub>MAXclad</sub>	(+)π <sub>Oclad</sub>	(+)W <sub>loading</sub>	(+)DI <sub>EPA:C</sub>
(-)EPA <sub>Mclad</sub>	(-)EPA <sub>Mclad</sub>	(-)EPA <sub>Mclad</sub>	(+)π <sub>MAXclad</sub>	(+)π <sub>MAXclad</sub>	(+)π <sub>MAXclad</sub>
(+)GR <sub>EPA:C</sub>	(+)GR <sub>EPA:C</sub>	(+)GR <sub>EPA:C</sub>	(+)DI <sub>EPA:C</sub>	(-)CB <sub>EPA:C</sub>	(-)CB <sub>EPA:C</sub>
Mesotrophic					
JAN	FEB	MAR	APR	MAY	JUN
(+)W <sub>loading</sub>					
(-)EPA <sub>Mclad</sub>	(+)DI <sub>EPA:C</sub>	(-)P <sub>Oclad</sub>	(-)P <sub>Oclad</sub>	(-)P <sub>Oclad</sub>	(-)P <sub>Oclad</sub>
(+)DI <sub>EPA:C</sub>	(-)EPA <sub>Mclad</sub>	(+)π <sub>MAXclad</sub>	(+)π <sub>MAXclad</sub>	(+)π <sub>MAXclad</sub>	(+)π <sub>MAXclad</sub>
(+)π <sub>MAXclad</sub>	(+)π <sub>MAXclad</sub>	(+)DI <sub>EPA:C</sub>	(+)W <sub>YPotemp</sub>	(+)W <sub>YPotemp</sub>	(-)EPA <sub>Mclad</sub>
(-)DHA <sub>Mcope</sub>	(-)DHA <sub>Mcope</sub>	(-)EPA <sub>Mclad</sub>	(+)W <sub>EPItemp</sub>	(+)GR <sub>EPA:C</sub>	(+)DHA <sub>Ocope</sub>
JUL	AUG	SEP	OCT	NOV	DEC
(+)W <sub>loading</sub>	(-)W <sub>loading</sub>	(+)W <sub>loading</sub>	(+)W <sub>loading</sub>	(+)W <sub>loading</sub>	(+)W <sub>loading</sub>
(-)P <sub>Oclad</sub>	(+)π <sub>MAXclad</sub>	(+)π <sub>MAXclad</sub>	(+)π <sub>MAXclad</sub>	(+)DI <sub>EPA:C</sub>	(+)DI <sub>EPA:C</sub>
(+)π <sub>MAXclad</sub>	(-)P <sub>Oclad</sub>	(-)P <sub>Oclad</sub>	(+)DI <sub>EPA:C</sub>	(+)π <sub>MAXclad</sub>	(-)EPA <sub>Mclad</sub>
(-)EPA <sub>Mclad</sub>	(+)π <sub>MAXclad</sub>				
(+)GR <sub>EPA:C</sub>	(+)GR <sub>EPA:C</sub>	(+)W <sub>YPotemp</sub>	(-)P <sub>Oclad</sub>	(+)W <sub>YPotemp</sub>	(-)P <sub>Ocope</sub>
Eutrophic					
JAN	FEB	MAR	APR	MAY	JUN
(+)DI <sub>EPA:C</sub>					
(+)T <sub>Nclad</sub>	(+)T <sub>Nclad</sub>	(+)π <sub>MAXclad</sub>	(+)π <sub>MAXclad</sub>	(+)π <sub>MAXclad</sub>	(+)T <sub>Pclad</sub>
(-)EPA <sub>Mclad</sub>	(-)CB <sub>EPA:C</sub>	(-)CB <sub>EPA:C</sub>	(+)T <sub>Nclad</sub>	(+)T <sub>Nclad</sub>	(-)CB <sub>EPA:C</sub>
(-)CB <sub>EPA:C</sub>	(-)EPA <sub>Mclad</sub>	(-)EPA <sub>Mclad</sub>	(-)CB <sub>EPA:C</sub>	(+)T <sub>Pclad</sub>	(+)N <sub>Mclad</sub>
(+)N <sub>Mclad</sub>	(+)π <sub>MAXclad</sub>	(+)T <sub>Pclad</sub>	(+)T <sub>Pclad</sub>	(-)CB <sub>EPA:C</sub>	(+)π <sub>MAXclad</sub>
JUL	AUG	SEP	OCT	NOV	DEC
(+)DI <sub>EPA:C</sub>					
(+)π <sub>MAXclad</sub>	(+)π <sub>MAXclad</sub>	(+)π <sub>MAXclad</sub>	(-)EPA <sub>Mclad</sub>	(-)EPA <sub>Mclad</sub>	(+)T <sub>Nclad</sub>
(-)EPA <sub>Mclad</sub>	(-)EPA <sub>Mclad</sub>	(-)EPA <sub>Mclad</sub>	(+)π <sub>MAXclad</sub>	(-)CB <sub>EPA:C</sub>	(-)EPA <sub>Mclad</sub>
(-)CB <sub>EPA:C</sub>	(-)CB <sub>EPA:C</sub>	(-)CB <sub>EPA:C</sub>	(-)CB <sub>EPA:C</sub>	(+)π <sub>MAXclad</sub>	(-)CB <sub>EPA:C</sub>
(+)T <sub>Pclad</sub>	(-)DHA <sub>Mcope</sub>	(+)N <sub>Ocope</sub>	(+)N <sub>Mclad</sub>	(+)T <sub>Nclad</sub>	(+)χ <sub>Nclad</sub>

availability in diatoms ( $DI_{DHA:C}$ ) as well as the copepod minimum somatic DHA ( $DHA_{Mcope}$ ). Unlike cladocerans, copepods were designed to accumulate DHA, and so where EPA-related parameters were of importance to cladocerans, DHA-parameters are to copepods. Interestingly, green algae EPA content ( $GR_{EPA:C}$ ), exerts positive control on copepod biomass in several months. Our model parameterization treats green algae as extremely rich sources of PUFAs, relatively poor source of EPA, and completely devoid of DHA. It stands to reason that despite lacking DHA, the superior HUFA bioconversion capacity of copepods allows them to meet both their EPA and DHA requirements. Likewise, whereas cladoceran somatic growth is sensitive to available P, copepods are postulated to have higher N content. Thus, both optimal and minimum somatic N ( $N_{Ocope}$  and  $N_{Mcope}$ , respectively) are negatively associated with the copepod biomass. Diatom EPA ( $DI_{EPA:C}$ ) is negatively related to copepod biomass in April and July. The negative influence may stem from the positive impact of the same parameter on

cladoceran biomass, which in turn renders competitive handicap to copepods.

**Alternate loading scenarios.** A similar regression analysis in the oligotrophic environment illustrates many of the same patterns and influential parameters as in the mesotrophic setting. Nutrient loading ( $W_{loading}$ ) remains one of the most influential factors for both cladocerans and copepods. Dependence on recycled nutrients is an interesting difference between the two zooplankton functional groups. Copepods are positively influenced by cladoceran P ( $T_{Pclad}$ ) and their own N turnover rate ( $T_{Ncope}$ ; see Table 5), whereas cladocerans do not demonstrate a strong reliance upon the recycling patterns; at least, as manifested by the top five parameters presented in Table 4. Under eutrophic conditions, however, there is a substantial shift in the factors driving animal growth. Cladocerans are no longer influenced by nutrient loading, but rather the most influential parameter across all months is the EPA content in diatoms ( $DI_{EPA:C}$ ; see Table 4). Both P and N turnover

**Table 5**  
Multiple regression analysis of the most influential model parameters for copepod biomass listed by month across oligotrophic, mesotrophic, and eutrophic conditions.

Oligotrophic					
JAN	FEB	MAR	APR	MAY	JUN
(+) $W_{loading}$	(+) $W_{loading}$	(+) $W_{loading}$	(+) $W_{loading}$	(-) $N_{Mcope}$	(-) $N_{Mcope}$
(-) $N_{Mcope}$	(-) $N_{Mcope}$	(-) $N_{Mcope}$	(-) $N_{Mcope}$	(+) $W_{loading}$	(+) $W_{loading}$
(-) $DHA_{Mcope}$	(-) $DHA_{Mcope}$				
(+) $T_{Pclad}$	(-) $EPA_{Oclad}$				
(+) $DI_{DHA:C}$	(-) $m_{cope}$	(-) $N_{Oclad}$	(-) $N_{Oclad}$	(-) $EPA_{Oclad}$	(-) $N_{Oclad}$
JUL	AUG	SEP	OCT	NOV	DEC
(-) $N_{Mcope}$	(-) $N_{Mcope}$	(+) $DET_{DHA:C}$	(-) $T_{Pclad}$	(+) $P_{Mcope}$	(+) $T_{Mclad}$
(+) $W_{loading}$	(+) $W_{loading}$	(+) $h_{EPAcope}$	(+) $GR_{EPA:C}$	(-) $EPA_{Oclad}$	(-) $W_{diffusivity}$
(-) $DHA_{Mcope}$	(-) $DHA_{Mcope}$	(+) $P_{Mclad}$	(+) $DHA_{Mclad}$	(+) $T_{DHAclad}$	(+) $GR_{EPA:C}$
(-) $N_{Oclad}$	(+) $T_{Pclad}$	(+) $P_{Mcope}$	(-) $J_{PUFAgr}$	(-) $W_{diffusivity}$	(-) $W_{loading}$
(-) $EPA_{Oclad}$	(-) $N_{Oclad}$	(+) $EPA_{Ocope}$	(+) $T_{Ncope}$	(+) $h_{EPAcope}$	(+) $DHA_{Mclad}$
Mesotrophic					
JAN	FEB	MAR	APR	MAY	JUN
(+) $W_{loading}$	(+) $DI_{DHA:C}$				
(+) $DI_{DHA:C}$	(+) $DI_{DHA:C}$	(+) $DI_{DHA:C}$	(-) $N_{Ocope}$	(+) $\pi_{MAXcope}$	(+) $\pi_{MAXcope}$
(-) $DHA_{Mcope}$	(-) $DHA_{Mcope}$	(-) $DHA_{Mcope}$	(-) $N_{Mcope}$	(-) $P_{Ocope}$	(+) $W_{loading}$
(+) $GR_{EPA:C}$	(+) $GR_{EPA:C}$	(+) $\pi_{MAXcope}$	(+) $\pi_{MAXcope}$	(+) $DI_{DHA:C}$	(-) $DHA_{Mcope}$
(+) $\pi_{MAXcope}$	(-) $N_{Oclad}$	(-) $N_{Mcope}$	(-) $DI_{EPA:C}$	(+) $GR_{EPA:C}$	(-) $N_{Oclad}$
JUL	AUG	SEP	OCT	NOV	DEC
(+) $DI_{DHA:C}$	(+) $W_{loading}$	(+) $W_{loading}$	(+) $W_{loading}$	(+) $W_{loading}$	(+) $W_{loading}$
(+) $\pi_{MAXcope}$	(+) $DI_{DHA:C}$	(-) $N_{Mcope}$	(-) $N_{Mcope}$	(+) $DI_{DHA:C}$	(+) $DI_{DHA:C}$
(+) $W_{loading}$	(-) $N_{Mcope}$	(+) $\pi_{MAXcope}$	(+) $DI_{DHA:C}$	(-) $N_{Mcope}$	(-) $DHA_{Mcope}$
(-) $DI_{EPA:C}$	(+) $\pi_{MAXcope}$	(+) $DI_{DHA:C}$	(+) $\pi_{MAXcope}$	(+) $\pi_{MAXcope}$	(+) $\pi_{MAXcope}$
(-) $DHA_{Mcope}$	(-) $N_{Oclad}$	(-) $N_{Oclad}$	(-) $N_{Oclad}$	(-) $DHA_{Mcope}$	(-) $N_{Mcope}$
Eutrophic					
JAN	FEB	MAR	APR	MAY	JUN
(+) $DI_{EPA:C}$	(+) $DI_{EPA:C}$	(+) $DI_{EPA:C}$	(+) $DI_{EPA:C}$	(+) $DI_{DHA:C}$	(+) $DI_{DHA:C}$
(-) $DHA_{Mcope}$	(-) $DHA_{Mcope}$	(-) $DHA_{Mcope}$	(-) $DI_{DHA:C}$	(-) $DI_{EPA:C}$	(-) $DHA_{Mcope}$
(-) $EPA_{Mclad}$	(+) $\pi_{MAXclad}$	(+) $DI_{DHA:C}$	(-) $DHA_{Mcope}$	(-) $DHA_{Mcope}$	(+) $T_{Nclad}$
(+) $\pi_{MAXclad}$	(+) $DI_{DHA:C}$	(+) $P_{Mclad}$	(-) $N_{Mcope}$	(-) $N_{Mcope}$	(-) $N_{Mcope}$
(-) $CB_{EPA:C}$	(+) $P_{Mclad}$	(-) $N_{Mcope}$	(+) $T_{Nclad}$	(+) $N_{Mclad}$	(+) $N_{Mclad}$
JUL	AUG	SEP	OCT	NOV	DEC
(+) $DI_{DHA:C}$	(+) $DI_{DHA:C}$	(+) $DI_{DHA:C}$	(-) $DHA_{Mcope}$	(+) $DI_{EPA:C}$	(+) $DI_{EPA:C}$
(+) $T_{Nclad}$	(-) $DHA_{Mcope}$	(+) $DI_{EPA:C}$	(+) $DI_{DHA:C}$	(-) $DHA_{Mcope}$	(-) $DHA_{Mcope}$
(-) $DHA_{Mcope}$	(+) $T_{Nclad}$	(-) $DHA_{Mcope}$	(+) $DI_{EPA:C}$	(+) $DI_{DHA:C}$	(+) $\pi_{MAXclad}$
(-) $J_{PUFAcb}$	(+) $DI_{EPA:C}$	(+) $T_{Nclad}$	(-) $EPA_{Mcope}$	(-) $EPA_{Mclad}$	(-) $N_{Mcope}$
(-) $N_{Mcope}$	(-) $J_{PUFAdi}$	(-) $J_{PUFAdi}$	(+) $\pi_{MAXclad}$	(+) $T_{Nclad}$	(+) $DI_{DHA:C}$

rates ( $T_{Nclad}$  and  $T_{Pclad}$ ) exhibit a positive influence on cladoceran biomass, most likely reflecting the capacity of the released material from zooplankton metabolism to modulate the amplitude of phytoplankton-zooplankton dynamics. Similarly, copepods are significantly influenced by diatom DHA ( $DI_{DHA:C}$ ) and EPA content ( $DI_{EPA:C}$ ; see Table 5). Our calibration parameterizes diatoms as a rich source of DHA, but an even richer source of EPA. Copepods respond positively to both resources, and are most likely bioconverting much of their assimilated EPA into DHA.

**Phytoplankton.** Being the most abundant and nutritionally richer food source, diatoms demonstrate a tight relationship with the two zooplankton functional groups (see Table 1 in ESM). In particular, the HUFA-rich diatoms more efficiently support higher zooplankton growth and thus more intense herbivorous grazing. Likewise, a higher cladoceran growth rate ( $\pi_{MAXclad}$ ) yields a lower diatom abundance. Similarly, the lower the likelihood for copepods to experience mineral N limitation (low  $N_{Mcope}$ ), the greater the

control exerted on diatoms due to their feeding activity. Positively influential factors include DHA ( $DHA_{Ocope}$ ), N ( $N_{Mcope}$  and  $N_{Ocope}$ ) and P ( $P_{Mclad}$ ) parameters that stand to limit zooplankton growth upon increase. Bioconversion efficiency parameters controlling EPA-DHA ( $\rho$ ) and PUFA-EPA ( $\nu$ ) transformations are negatively and positively influential, respectively. This result suggests that the alleviation of nutritional limitation via internal bioconversion mechanisms can accentuate the grazing stress on diatoms. Our multiple regression analysis provided similar results for green algae (see Table 1 in ESM). One interesting pattern across both diatoms and greens is also the negative influence of copepod moult fraction ( $m_{cope}$ ). According to our submodel, a higher moult fraction results in higher recycled material in particulate form, and thus less readily available recycled material for phytoplankton uptake.

Despite some similarities to the aforementioned results, cyanobacteria regression analysis (see Table 1 in ESM) revealed stark differences. For example, cyanobacteria are the only producer

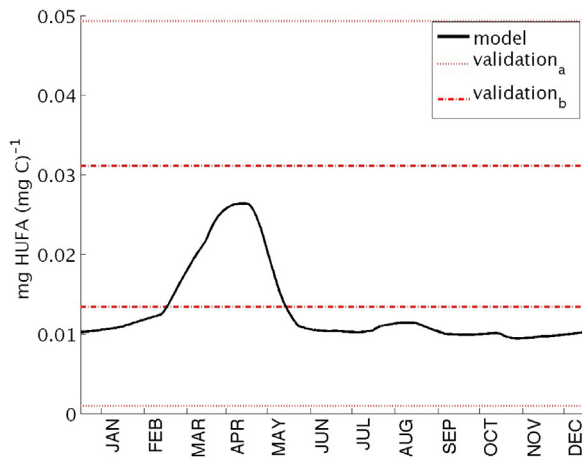


**Fig. 7.** Total cladoceran HUFA variability throughout the annual cycle, shown against total HUFA validation limits approximated from (a) Wainman et al. (1993), Falk-Petersen et al. (1987), and Ravet et al. (2010); (b) Smyntek et al. (2008) and Ravet et al. (2010).

species in which nutrient loading is not a primary regulatory factor of their biomass levels. Possessing inferior P kinetics, cyanobacteria are apparently less responsive to the variability of external P subsidies into the system. Unlike diatoms and greens, epilimnetic water temperature becomes an important negatively related factor in late summer. While this result seems counterintuitive, as cyanobacteria are assumed to be favoured by warmer conditions, it can be partly explained by the predominance of the temperature-dependent basal metabolic losses over the net cyanobacteria growth in P limiting environments during the stratified period. Finally, it seems that zooplankton N recycling can shape the competition patterns of cyanobacteria with other producer species. Increased N recycling (e.g., high  $T_{Nclad}$  and  $\chi_{Nclad}$ ) reduces the cyanobacteria competitive edge in N-kinetics. Perplexingly, however, the same N excretion rate that was negatively influential becomes positive if it stems from cladocerans. This may suggest a differential total impact of the two zooplankton groups when we discount their grazing control. That is, copepods are parameterized as selective feeders that have the capacity to diminish cyanobacteria contribution to their diet, whereas cladocerans are modelled as filter feeders.

**Seasonal sensitivity functions.** We created sensitivity functions that depict the variability in the importance of the different parameters during the annual cycle, which can also be indicative of the nature and the interconnectedness of the driving forces that control zooplankton dynamics. Using results from the cladoceran regression analysis, we focused on the maximum cladoceran growth rate against parameters representing somatic resource thresholds, seston nutritional content, and animal excretion rates. Grazers such as cladocerans with low C:P are highly sensitive to P availability. Plotting the standardized regression coefficients of the physiological parameters that characterize their somatic requirements for P ( $P_{Mclad}$  and  $P_{Octad}$ ) reveals a negative relationship between the optimal somatic P and cladoceran biomass (see Fig. 8a, d, g), implying that a higher optimal somatic P could be a disadvantage for cladoceran growth. While this qualitative response is manifested across all three trophic environments, we note that its magnitude decreases in the eutrophic state, coinciding with the emergence of P turnover rate as the most influential factor of cladoceran biomass (see Fig. 8g). On the other hand, a lower minimum EPA requirement renders a competitive advantage for cladoceran growth across all three trophic states (Fig. 8b, d, f). Our analysis suggests that the turnover rates or the EPA amount allotted to hormone production play a minor role on cladoceran biomass variability. Our analysis also shows that the EPA minimum requirement is

quantitatively as important as the maximum growth assigned to the cladoceran functional group. A similar conclusion could be drawn about the optimum EPA somatic content in the eutrophic environment, whereas the role of the latter parameter is being downplayed in the oligo- and mesotrophic settings.

We also note the counterintuitively positive nature of the relationship between cladoceran biomass and minimum P content. While a lower  $P_{Mclad}$  should render competitive advantage to a cladoceran, our analysis consistently suggests a positive causal association. One plausible explanation may be related to the implications of the P somatic content on the strength of the recycling loop. Namely, a higher minimum P threshold postulates an animal body richer in P, which in turn promotes zooplankton recycling (e.g., excretion rates, bacterial decomposition of dead tissues). The absence of such a positive relationship between the two HUFA minimum thresholds ( $EPA_{Mclad}$  and  $DHA_{Mclad}$ ) stems from our assumption that the corresponding recycled fluxes are permanently lost from the system (Perhar et al., 2012c). We also highlight the importance of diatom EPA content in the eutrophic scenario (Fig. 8f) and the positive control exerted from both  $DI_{EPA:C}$  and  $GR_{EPA:C}$  in the mesotrophic environment.

### 3.3. Homeostatic response and nutrient recycling

In the context of phytoplankton modeling, one approach to explicitly consider the role of algal nutrient quotas is to define absolute minimum and maximum quota limits (e.g., Droop, 1968), whereby cellular function is crippled below the minimum quota, and the maximum is constrained by vacuole volume. Drawing parallels with zooplankton modeling, we note that a minimum can be defined for somatic resource pools (i.e., resource threshold concentration below which metabolic functions slow down), but a rigid upper limit is debatable. Instead, we have chosen to adopt an optimal threshold, above which accrual can continue but at no gain to the consumer growth. Under nutrient enrichment conditions though, our experience has been that zooplankters were amassing nutrients in their storage reserves well above their parameterized norms and substantially muted any dynamic response the system may have taken. An alternative strategy would have been to cripple animal somatic growth or grazing rate as internal resources exceed the optimal threshold. If grazers are consistently accruing more resources than required, they could be considered *fat* or *sluggish*, and as such their overall fitness and competitive ability are likely to decrease.

In the present study, our handling of aggressive accrual was to delineate two excretion modes: *regular* and *venting*. We expect both the parameterized value of *venting* mode and the excretion response to impact ecosystem dynamics. The tightly bound relationship between zooplankton and aquatic nutrients is very sensitive in the present study, due to the mechanistic post-gut processing of matter in zooplankton, in a food web context. In contrast, contemporary studies focusing on individual based dynamics may not fully consider a dynamic environment (e.g., Anderson et al., 2005), and those with dynamic nutrient environments may not consider dynamic food processing in zooplankton (e.g., Arhonditsis and Brett, 2005a,b). Further, although outside the scope of the present study, we note a Holling type II response curve may represent a more appropriate somatic response, one which is truly dynamic and may mitigate any artifacts introduced by the abrupt shift from regular excretion to *venting* excretion (see Fig. 1b in ESM). Another philosophical debate involves the regulatory release when internal substrates are below the minimum threshold. Empirical evidence suggests excretion remains active under nutrient limiting scenarios (DeMott et al., 1998); dynamic substrate handling utilizing a Holling type II response has been shown to regulate grazer

functioning across a dynamic environment (e.g., Perhar et al., 2012c).

Earlier work with the original model construct (see Arhonditsis and Brett, 2005b; Zhao et al., 2008b) has demonstrated the phytoplankton-zooplankton interface to destabilize with increasing allochthonous loading, illustrating patterns qualitatively similar to those referred to as paradox of enrichment (Rosenzweig, 1971). The basic premise being as nutrient loading increases, phytoplankton experiences unconstrained growth, which in turn triggers high amplitude prey-predator oscillations, unsustainable zooplankton growth, and eventually population crash (Rosenzweig, 1971; Gilpin and Rosenzweig, 1972). Recently, Roy and Chattopadhyay (2007) summarized scenarios in which the paradox of enrichment is not expected and systems with inedible and/or unpalatable prey are one such example. Our results show a dramatic shift to cyanobacteria-dominated algae under nutrient enrichment, but the population response remains smooth and fails to demonstrate the instability experienced by the host model under similar circumstances (see Arhonditsis and Brett, 2005b). One plausible explanation for the more static response of the upgraded model may be the increased complexity and additional parameterization introduced by our growth submodel, mitigating the destabilizing forces (Perhar et al., 2012c). To consolidate this hypothesis, we tested the impact of prey edibility and palatability on enrichment destabilization and compared our base enrichment scenario to one in which all phytoplankton functional groups were parameterized with ideal palatability (i.e., perfect morphology). Post spring bloom dynamics were more turbulent than our base enrichment condition (see Fig. 9b and c), but were significantly muted compared to the host model's enrichment scenario. We

also gauged the impacts of resource handling by the zooplankters on system destabilization. Interestingly, changing zooplankton venting mode from  $0.1 \text{ day}^{-1}$  to  $0.9 \text{ day}^{-1}$  demonstrated significantly stronger post-spring bloom limit cycles, and yielded a more dynamic algal biomass response throughout the annual cycle. Thus, the homeostatic regulation of nutrient accrual into and excreted material from the animal body may apparently be one of the critical mechanisms that modulate system response to nutrient enrichment. Importantly, our results highlight the causal link between the maintenance of somatic quotas and the differential nutrient recycling as an important mechanism for reconciling the controversial hypothesis that the abundance of natural resources is essentially a destructive force that would destabilize community dynamics.

### 3.4. Nutrient cycles in Lake Washington

The simulated nitrogen and phosphorus cycles in the epilimnion are presented in Figs. 10 for the stratified period (May 31st–October 2nd). As in Arhonditsis and Brett (2005b), external loading was based on mean annual nutrient cycles over a 10-year period for all important Lake Washington tributaries, and an epilimnetic volume of  $0.81 \text{ km}^3$  (Arhonditsis et al., 2003) was used. In the stratified period, our model considers fluvial and atmospheric total nitrogen loading of  $151 \times 10^3 \text{ kg}$ , with ammonium and nitrate loading supplies contributing  $5.5 \times 10^3 \text{ kg}$  and  $69 \times 10^3 \text{ kg}$ , respectively. The system loses  $64 \times 10^3 \text{ kg}$ ,  $2.5 \times 10^3 \text{ kg}$ , and  $20 \times 10^3 \text{ kg}$  of total nitrogen, ammonium, and nitrate, respectively through the Lake Union Ship Canal outflow. Total phosphorus loading for the same period is  $12.1 \times 10^3 \text{ kg}$ , while  $1.0 \times 10^3 \text{ kg}$  and  $3.6 \times 10^3 \text{ kg}$  enter

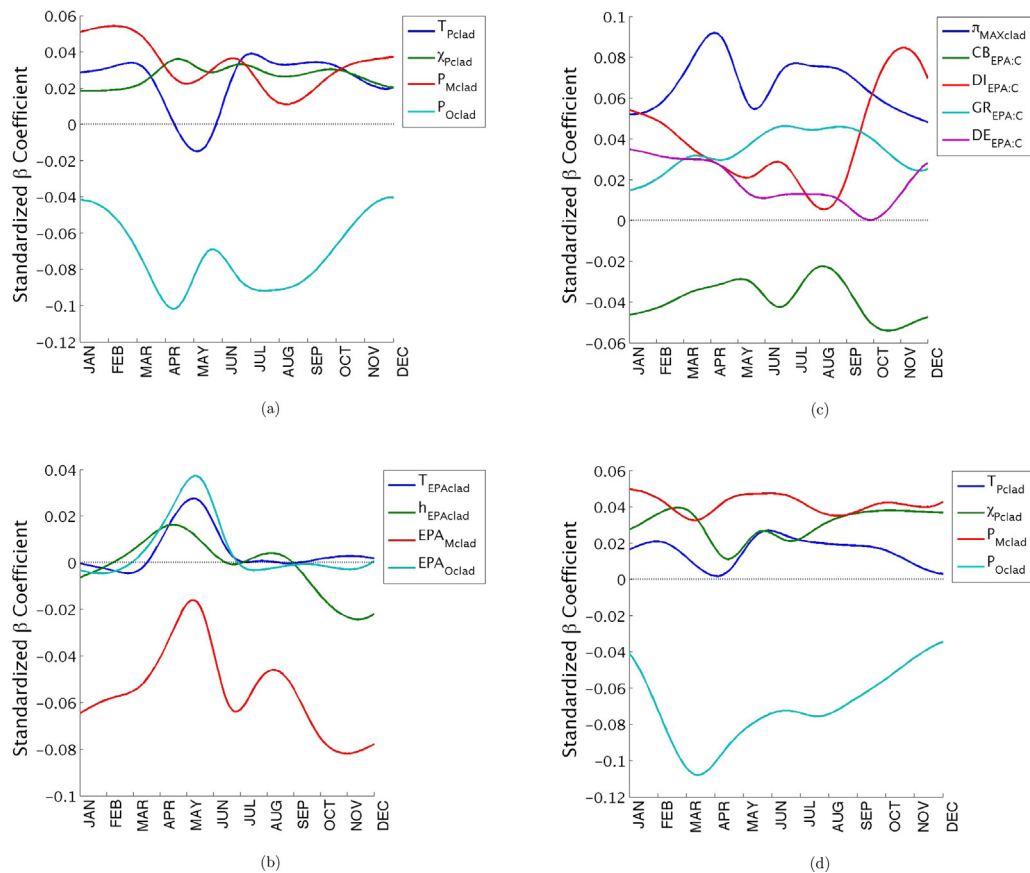


**Fig. 8.** Seasonal sensitivity of cladoceran biomass to P (a, d, g), EPA (b, e, h), and seston HUFA (c, f, i) submodel parameters across oligotrophic, mesotrophic, and eutrophic conditions; functions depict regression  $\beta$  values.

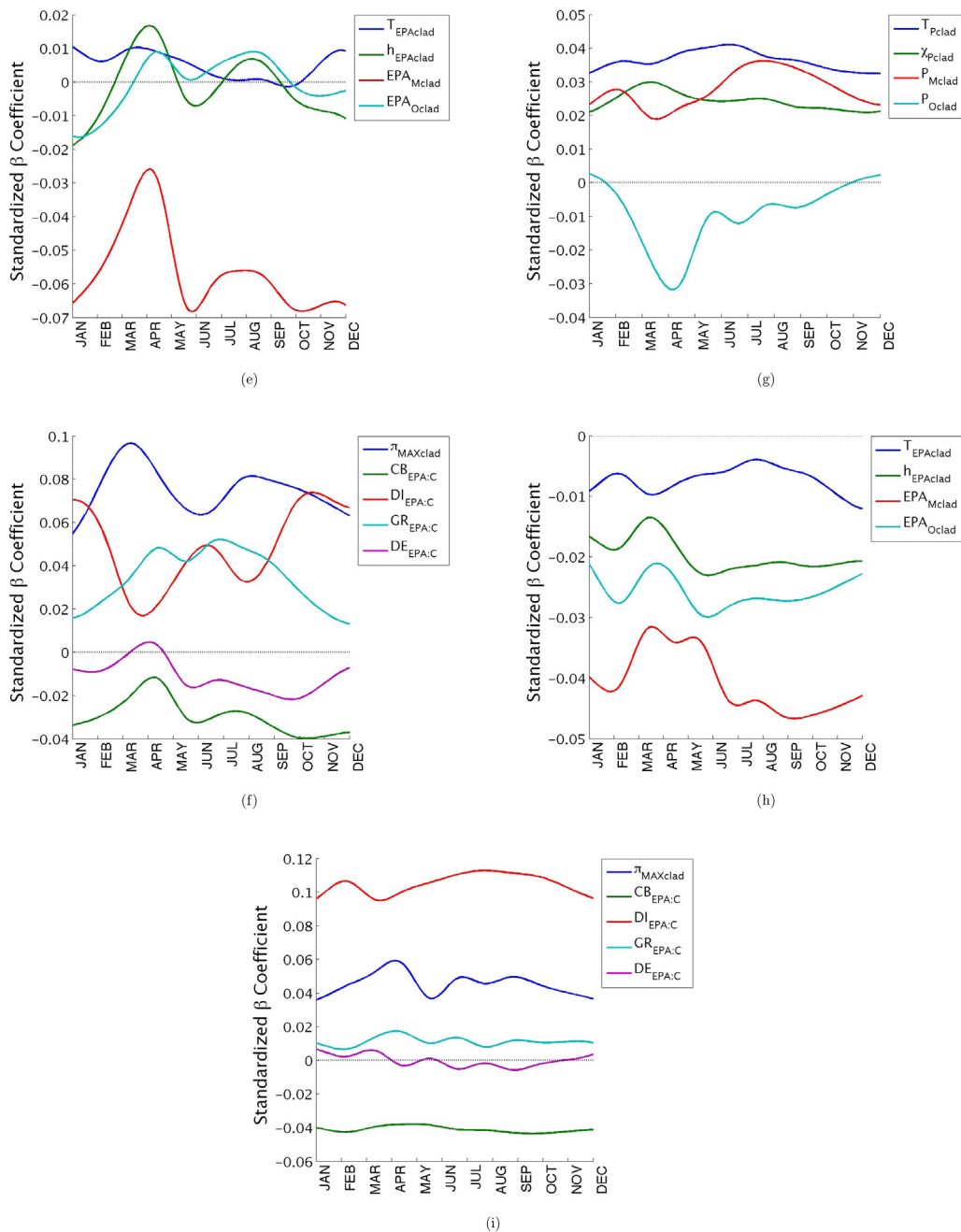
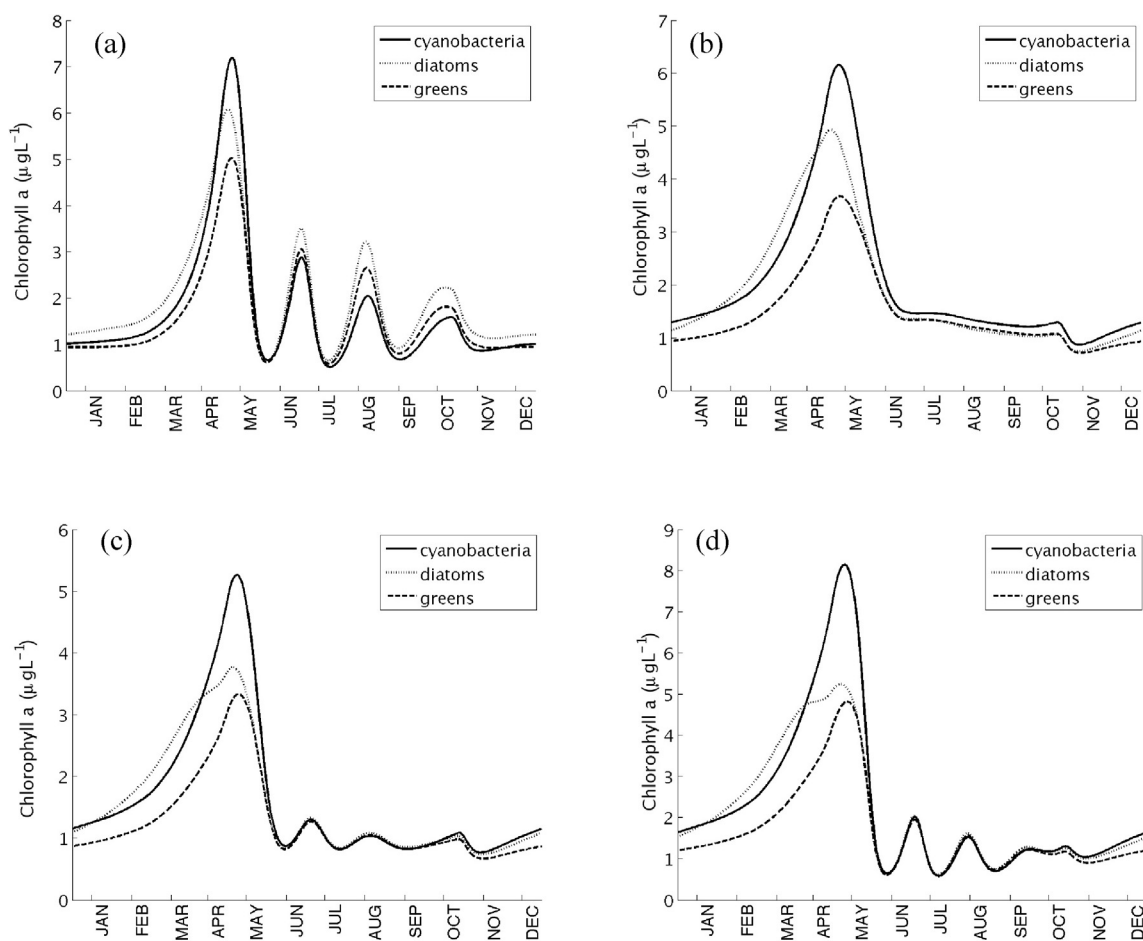


Fig. 8. (Continued).

as DOP and phosphate, respectively. Phosphorus outflow losses are  $1.8 \times 10^3$  kg,  $0.94 \times 10^3$  kg, and  $0.63 \times 10^3$  kg for total phosphorus, DOP and phosphate, respectively. Herbivorous zooplankton grazing removes  $160 \times 10^3$  kg and  $11.7 \times 10^3$  kg of N and P, respectively, while detritivorous grazing removes  $154 \times 10^3$  kg and  $12.3 \times 10^3$  kg of N and P, respectively. Net phytoplankton growth (uptake – basal metabolism) removes  $113 \times 10^3$  kg N and  $10.9 \times 10^3$  kg P during the stratified period.

The philosophy behind our current approach to modeling zooplankton is a departure from previous studies utilizing pre-gut regulatory mechanisms (e.g., Arhonditsis and Brett, 2005a; Perhar and Arhonditsis, 2009; Perhar et al., 2012c). Grazers utilizing pre-gut regulation retain portions of grazed seston such that ingested food meets somatic requirements. Discrimination criteria range from stoichiometric (e.g., food P:C content) to biochemical (e.g.,

fatty and amino acid content) and morphological (e.g., ingestibility and digestibility) constraints (Perhar and Arhonditsis, 2009). In the case of low C:P grazers, like *Daphnia*, phosphorus-limiting conditions may be accentuated as non-limiting nutrients are preferentially recycled while phosphorus is retained (Arhonditsis and Brett, 2005b). According to stoichiometric theory, ingested food is retained at stoichiometric ratios similar to somatic quotas (Elser and Urabe, 1999). That is, grazers with low somatic C:P and C:N will recycle matter with higher C:P and C:N than grazers with high C:P and C:N (Arhonditsis and Brett, 2005b). While our zooplankton growth submodel retains elements of pre-gut discrimination, it is minimized in favour of post-gut nutrient processing. One consequence of relaxing pre-gut regulation (to the point of reflecting only morphological quality) is the increased bulk of matter passed from the grazing apparatus to the gut, reducing particulate matter



**Fig. 9.** Dynamic equilibria response of algal biomass to P enrichment. Compared to host model performance (Arhonditsis and Brett, 2005b) (a), the submodel yields a very smooth response to enrichment (b). Equally high food quality across all food sources induced post spring-bloom instability (c). Perturbations were further enhanced by more rapid approach to the recycling of phosphorus (d).

release from *sloppy feeding* (see Fig. 12). Another consequence is the additional dissolved organic release supplementing existing basal metabolic activities. As more non-limiting nutrients are released in dissolved form, we expect their residence time to increase (Arhonditsis and Brett, 2005b). In contrast to the approach used by Arhonditsis and Brett (2005a), our model considers dynamic zooplankton C:N and C:P ratios, both of which regulate the release of DON and DOP. In our integration and calibration of the submodel, we assigned byproducts of sloppy feeding entirely to particulate form, representing remnants of food particles subject to sinking and dissolution/hydrolysis. Further, basal metabolic releases of DON and DOP were supplemented with byproducts of biomass turnover and regulatory excretion. In the stratified period, our model produced zooplankton particulate releases of  $109 \times 10^3$  kg N and  $14 \times 10^3$  kg P, respectively. The corresponding non-particulate zooplankton releases of N and P were  $179 \times 10^3$  kg and  $4.6 \times 10^3$  kg. The stoichiometries of the recycled material reflect the preferential P retention in P-limited systems. Zooplankton particulate and non-particulate egestion N:P ratios are 7.6 and 38.9, respectively. In particular, N:P ratios of cladoceran particulate and non-particulate recycled matter were 6.0 and 47.1, while the corresponding N:P ratios from copepods for particulate and non-particulate matter were 13.1 and 22.

As expected, shifting the bulk of non-limiting nutrient recycling to dissolved form increases the DON fluxes, which may in turn boost heterotrophic bacterial activity (Kroer et al., 1994).

Specifically, while our predicted N dissolution rates ( $68 \times 10^3$  kg N) are fairly similar to those reported by the Arhonditsis and Brett (2005b) study ( $65 \times 10^3$  kg N), N mineralization ( $96 \times 10^3$  kg N) has significantly increased relative to the original estimates ( $57 \times 10^3$  kg N). In this regard, our analysis reinforces the notion that stoichiometrically driven zooplankton recycling may modulate the ambient nutrient levels, and thus can conceivably induce broader ecosystem alterations, such as the delicate resource competition among the typical residents of the epilimnetic algal assemblages (MacKay and Elser, 1998; Elser and Urabe, 1999; Ramin et al., 2012). Additionally, the stoichiometry of sedimenting material reported by Arhonditsis and Brett (2005b) of N:P= 11 (by weight per annum), has expectedly changed, as the bulk of recycled P is in particulate form, whereas N is primarily recycled in non-particulate form. According to our model,  $208 \times 10^3$  kg N and  $22 \times 10^3$  kg P are subject to sedimentation from the epilimnion over the period of 1 year. Our sedimentation N:P ratio of 9.4 is below the value reported in the host model, but well within the range of the values estimated by Edmondson and Lehman (1981). This finding downplays somewhat the assertion made by Arhonditsis and Brett (2005b) that the resurgence of P-rich *Daphnia* increased nitrogen sedimentation to the lake sediments, which in turn may have induced changes in the relative magnitude of nitrification/denitrification and their net effect (decrease of alkalinity by nitrification and increase by denitrification) could be associated with the increasing alkalinity trends in Lake Washington (Edmondson, 1994).

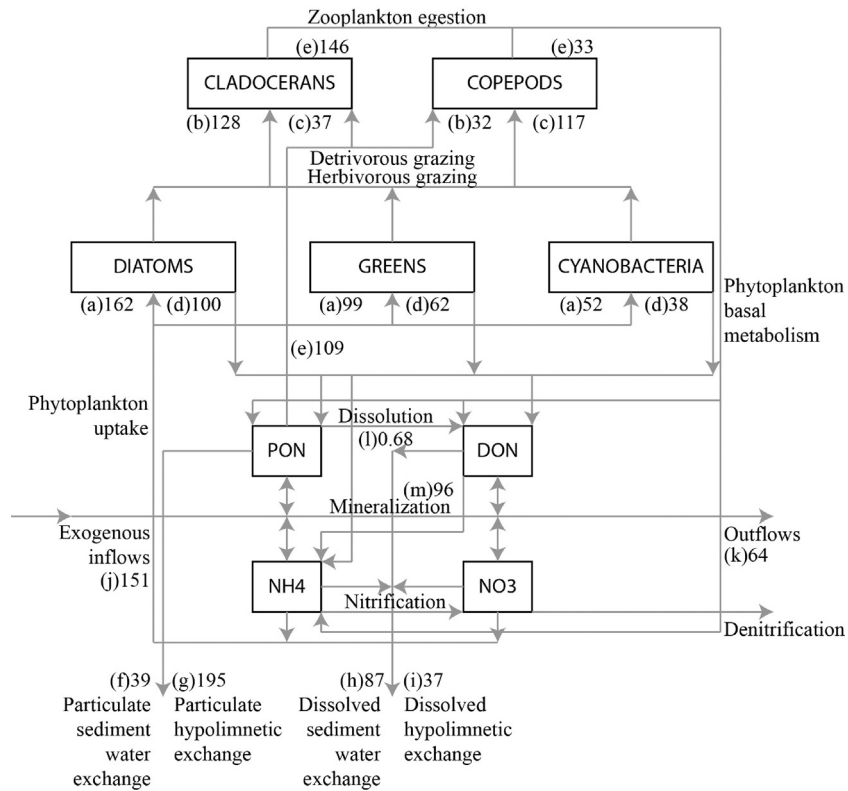


**Fig. 10.** Various nitrogen fluxes during the stratified period ranging from May 31st to October 1st in the epilimnion: (a) phytoplankton uptake, (b) herbivorous grazing, (c) detritivorous grazing, (d) phytoplankton basal metabolism, (e) zooplankton egestion and basal metabolism, (f) particulate sediment water exchange, (g) particulate hypolimnetic exchange, (h) dissolved sediment water exchange, (i) dissolved hypolimnetic exchange, (j) inflows, (k) outflows, (l) dissolution, (m) mineralization; shown in  $10^3$  kg.

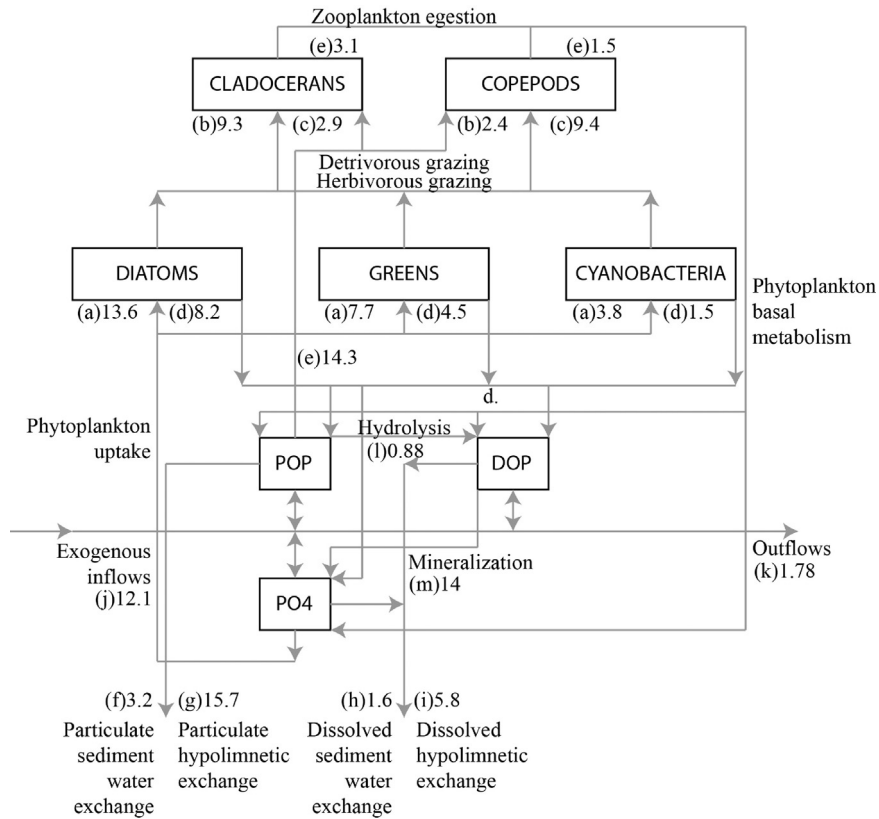
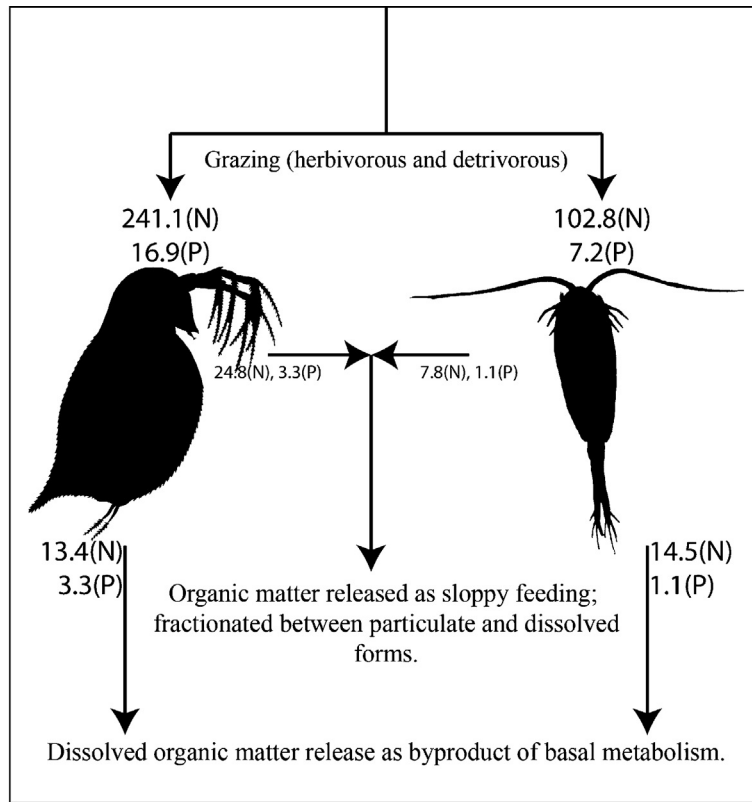
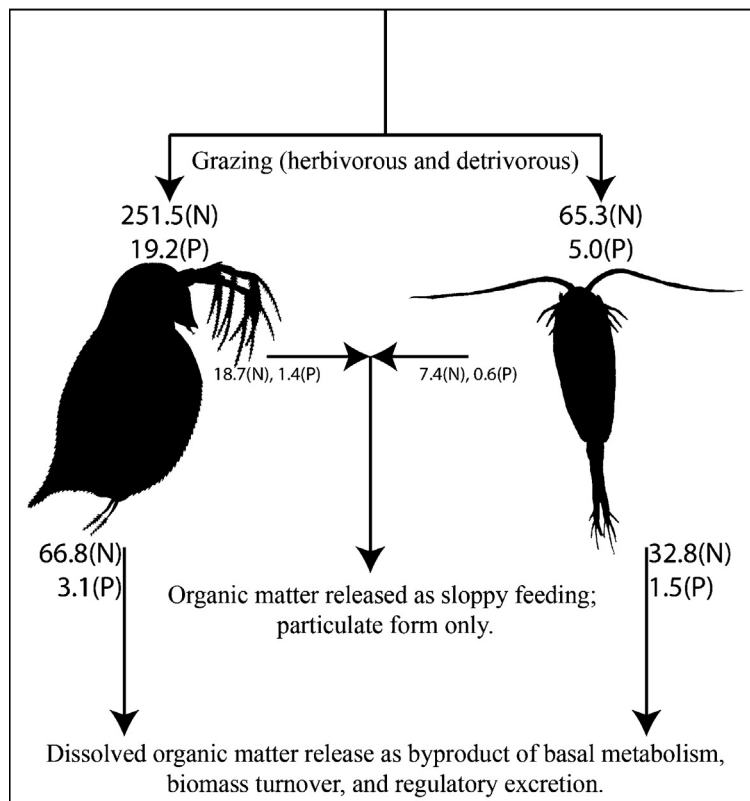


**Fig. 11.** Various phosphorus fluxes during the stratified period ranging from May 31st to October 1st in the epilimnion: (a) phytoplankton uptake, (b) herbivorous grazing, (c) detritivorous grazing, (d) phytoplankton basal metabolism, (e) zooplankton egestion and basal metabolism, (f) particulate sediment water exchange, (g) particulate hypolimnetic exchange, (h) dissolved sediment water exchange, (i) dissolved hypolimnetic exchange, (j) inflows, (k) outflows, (l) hydrolysis, (m) mineralization; shown in  $10^3$  kg.



(a) Pre-gut discrimination



(b) Post-gut discrimination

**Fig. 12.** (a and b) Conceptualized recycling consequences of pre- and post-gut absorption strategies. Pre-gut regulation as employed by Arhonditsis and Brett (2005a) releases particulate matter (as sloppy feeding) higher in non-limiting nutrient concentrations, and basal metabolic releases in dissolved form. Post-gut regulation as employed in our zooplankton growth submodel reduces pre-gut discrimination as well as egestion of non-limiting elements in particulate form. Homeostatic regulation is maintained via internal processes, and the bulk of non-limiting nutrient is returned to the system in dissolved form. Bulk grazed, egested, and excreted masses shown in  $10^3$  kg.

#### 4. Conclusions – future perspectives

In the present study, we have demonstrated the integration of a resource explicit zooplankton growth submodel into a complex management-oriented model. The upgraded eutrophication model provided a good representation of the key epilimnetic and hypolimnetic patterns in Lake Washington (USA). A satisfactory fit was obtained between simulated and observed monthly values for the major water quality variables (phytoplankton, phosphate, total phosphorus, total nitrogen, ammonium, dissolved oxygen). We have shown that both stoichiometric and HUFA-based somatic growth limitations can modulate the zooplankton biomass in mesotrophic environments. Our analysis qualitatively suggests that food abundance and mineral P limitation are critical factors of zooplankton growth under oligotrophic conditions, while HUFA limitation is more pronounced in eutrophic states. The homeostatic maintenance of somatic quotas and the differential nutrient recycling could be an important mechanism for reconciling the controversial hypothesis that the enrichment of natural ecosystems is a destructive force that would destabilize food web dynamics. Our zooplankton submodel downplays pre-gut regulation in favour of post-gut nutrient processing, projecting a substantial reduction of particulate matter release along with an increase of the residence time of the non-limiting elements. Grazers with high somatic C:P and C:N values are predicted to recycle dissolved matter with higher C:P and C:N than grazers with high C:P and C:N somatic ratios. Shifting the bulk of non-limiting nutrient recycling to dissolved form increases the DON fluxes, which in turn may augment the bacterially mediated mineralization activity.

There are inherent challenges to our approach in exploring *black-boxed* processes in zooplankton physiology. In previous work, we reported literature values for several parameters considered, but many still lack empirical information to properly constrain our zooplankton growth submodel. Compounds such as HUFAs interact with zooplankton tissue and extracellular components, but contemporary analytical techniques may only be able to quantify bulk assimilation. For example, metabolomics is a fairly recent advancement involving the study of endogenous low molecular weight metabolites (termed metabolomes) within cell tissues and biofluids (Viant, 2007). Patterns of endogenous metabolites in body fluids have been studied with hydrogen nuclear magnetic resonance (H NMR) spectroscopy (Nicholson et al., 1999). Often the first physiological response to anthropogenic stressors and natural daily events (Viant, 2007), the metabolome offers potential insights into physiological response to varying environmental conditions, and may usher in a new era of research. With the recent advances made in combining H NMR techniques with metabolomic response, detailed investigation of the differences in zooplankton metabolic response when exposed to HUFA rich and HUFA poor diets is possible. We believe guided experimentation of this type can address the parameter gaps in the literature.

Another interesting prospect of our modeling approach is the handling of temporal variability. We combine the food web dynamics of a plankton community with the physiology of an individual zooplankter. Solar radiation, temperature and exogenous loading are examples of environmental factors that vary with time, and in turn impact food web dynamics. Our modelled zooplankton physiology, however, remains constant throughout the annual cycle. That is, factors controlling somatic growth are not seasonally influenced. Zooplankton developmental stages, however, are expected to play a substantial role in controlling growth. Accounting for animal life history in our model in its present state would be difficult, but work done by Nisbet et al. (2000) on dynamic energy budgets (DEB) holds promise for such an incorporation. DEB models consider the ratio between animal surface area and volume, and the consequences of change over time. For example, in the body size

scaling of life history parameters in DEB theory, respiration rate decreases with increasing body size, while maximum grazing rate increases (Kooijman, 2010). Further, DEB theory delineates somatic structure and reserve compounds, such that assimilated matter is first stored as reserves, and then metabolized as needed. Combined, these traits can differentiate between juvenile grazers exhibiting high growth rates and negligible reproduction, and adults characterized by low growth rates and strong focus on reproduction.

#### Acknowledgments

This project has received funding support from the Natural Sciences and Engineering Research Council of Canada through a Doctoral Scholarship awarded to Gurbir Perhar and a Discovery Grant awarded to George Arhonditsis.

#### Appendix A. Supplementary data

Supplementary data associated with this article can be found, in the online version, at <http://dx.doi.org/10.1016/j.ecolmodel.2013.02.024>.

#### References

- Aita, M.N., Yamanaka, Y., Kishi, M.J., 2003. Effects of ontogenetic vertical migration of zooplankton on annual primary production – using NEMURO embedded in a general circulation model. *Fisheries Oceanography* 12, 284–290.
- Andersen, T., 1997. *Pelagic Nutrient Cycles*. Springer, New York.
- Anderson, T.R., Hessen, D.O., Elser, J.J., 2005. Metabolic stoichiometry and the fate of excess carbon and nutrients in consumers. *American Naturalist* 165, 1–15.
- Arhonditsis, G.B., Brett, M.T., 2005a. Eutrophication model for Lake Washington (USA). Part I. Model description and sensitivity analysis. *Ecological Modelling* 187, 140–178.
- Arhonditsis, G.B., Brett, M.T., 2005b. Eutrophication model for Lake Washington (USA). Part II. Model calibration and system dynamics analysis. *Ecological Modelling* 187, 179–200.
- Arhonditsis, G.B., Brett, M.T., Frodge, J., 2003. Environmental control and limnological impacts of a large recurrent spring bloom in Lake Washington, USA. *Environmental Management* 31, 603–618.
- Baird, M.E., 1999. Towards a verified mechanistic model of plankton population dynamics. PhD thesis, University of Warwick.
- Brett, M.T., Müller-Navarra, D.C., 1997. The role of highly unsaturated fatty acids in aquatic food web processes. *Freshwater Biology* 38, 483–499.
- Brewer, M.C., 1998. Mating behaviours of *Daphnia pulicaria*, a cyclic parthenogen: comparisons with copepods. *Philosophical Transactions of Royal Society of London B* 353, 805–815.
- Bryant, A.D., Heath, M., Gurney, W.S.G., Beare, D.J., Robertson, W., 1997. The seasonal dynamics of *Calanus finmarchicus*: development of a three-dimensional structured population model and application to the northern North Sea. *Journal of Sea Research* 38, 361–379.
- Bundy, M.H., Gross, T.F., Coughlin, D.J., Strickler, J.R., 1993. Quantifying copepod searching efficiency using swimming pattern and perceptible ability. *Bulletin of Marine Science* 53, 15–28.
- Conley, W.J., Turner, J.T., 1987. Omnivory by the coastal marine copepods *Centropages hamatus* and *Labidocera aestiva*. *Marine Ecology Progress Series* 21, 113–120.
- Coughlin, D.J., Strickler, J.R., Sanderson, B., 1992. Swimming and search behaviour in clownfish, *Amphiprion perideraion*, larvae. *Animal Behaviour* 44, 427–440.
- DeMott, W.R., Gulati, R.D., Siewertsen, K., 1998. Effects of phosphorus-deficient diets on the carbon and phosphorus balance of *Daphnia magna*. *Limnology and Oceanography* 43, 1147–1161.
- Dowling, N.A., Hall, S.J., Mitchell, J.G., 2001. Foraging kinematics of barramundi during early stages of development. *Journal of Fish Biology* 57, 337–353.
- Droop, M.R., 1968. Vitamin B<sub>12</sub> and marine ecology. IV. The kinetics of uptake, growth and inhibition in *Monochrysis lutheri*. *Journal of the Marine Biological Association of the United Kingdom* 48, 689–733.
- Edmondson, W.T., 1994. Sixty years of Lake Washington: a curriculum vitae. *Lake and Reservoir Management* 10, 75–84.
- Edmondson, W.T., Lehman, J.T., 1981. The effect of changes in the nutrient income on the condition of Lake Washington. *Limnology and Oceanography* 26, 1–29.
- Edwards, A.M., Yool, A., 2000. The role of higher predation in plankton population models. *Journal of Plankton Research* 22, 1085–1112.
- Elser, J.J., Urabe, J., 1999. The stoichiometry of consumer-driven nutrient recycling: theory, observations, and consequences. *Ecology* 80, 735–751.
- Falk-Petersen, S., Sargent, J.R., Tande, K.S., 1987. Lipid composition of zooplankton in relation to the Sub-Arctic food web. *Polar Biology* 8, 115–120.
- Fennel, W., Neumann, T., 2001. Coupling biology and oceanography in models. *AMBIO* 30, 232–236.

- Fiksen, O., Carlotti, F., 1998. A model of optimal life history and diel vertical migration in *Calanus finmarchicus*. *Sarsia* 83, 129–147.
- Fisher, R., Bellwood, D.R., Job, S.D., 2000. Development of swimming abilities in reef fish larvae. *Marine Ecology Progress Series* 202, 163–173.
- Frost, B.W., 1972. Effects of size and concentration of food particles on the feeding behavior of the marine planktonic copepod *Calanus pacificus*. *Limnology and Oceanography* 17, 805–815.
- Frost, B.W., 1975. A threshold feeding behavior in *Calanus pacificus*. *Limnology and Oceanography* 20, 263–266.
- Gilpin, M., Rosenzweig, M., 1972. Enriched predator–prey systems: theoretical stability. *Science* 177, 902–904.
- Gries, T., Jöhnk, K., Fields, K., Strickler, J.R., 1999. Size and structure of “footprints” produced by *Daphnia*: impact of animal size and density gradients. *Journal of Plankton Research* 21, 509–523.
- Ivlev, V.S., 1961. *Experimental Ecology of Nutrition of Fishes*. Yale University Press, New Haven, CT.
- Kleppel, G.S., Frazel, D., Pieper, R.E., Holliday, D.V., 1988. Natural diets of zooplankton off southern California. *Marine Ecology Progress Series* 49, 231–241.
- Kooijman, S.A.L.M., 2010. *Dynamic Energy Budget Theory for Metabolic Organisation*, 3rd ed. Cambridge University Press.
- Kroer, N., Jørgensen, N.O.G., Coffin, R.B., 1994. Utilization of dissolved nitrogen by heterotrophic bacterioplankton: a comparison of three ecosystems. *Applied and Environmental Microbiology* 60, 4116–4123.
- Lampert, W., 1989. The adaptive significance of diel vertical migration of zooplankton. *Functional Ecology* 3, 21–27.
- Lonsdale, D.J., Heinle, D.R., Siegfried, C., 1979. Carnivorous feeding by the adult calanoid copepod *Acartia tonsa* Dana. *Journal of Experimental Marine Biology and Ecology* 36, 235–248.
- MacKay, N.A., Elser, J.J., 1998. Factors potentially preventing trophic cascades: food quality, invertebrate predation, and their interaction. *Limnology and Oceanography* 43, 339–347.
- Mayer, D.G., Butler, D.G., 1993. Statistical validation. *Ecological Modelling* 68, 21–32.
- Mooij, W.M.D.T., Jeppesen, E., Arhonditsis, G.B., Belolipetsky, P.V., Chitamwebwa, D.B.R., Degermendzhy, A.G., DeAngelis, D.L., De Senerpont Domis, L.N., Downing, A.S., Elliott Jr., J.A., Fragoso, C.R., Gaedke, U., Genova, S.N., Gulati, R.D., Ha kanson, L., Hamilton, v. Hipsey, M.R., 't Hoen, J., Hulsmann, S., Los, F.H., Makler-Pick, V., Petzoldt, T., Prokopkin, v. Rinke, K., Schep, S.A., Tominaga, K., Van Dam, A.A., Van Nes, E.H., Wells, S.A., JansE, J.H., 2010. Challenges and opportunities for integrating lake ecosystem modelling approaches. *Aquatic Ecology* 44, 633–667.
- Mullin, M.M., Stewart, E.F., Fuglister, F.J., 1975. Ingestion by planktonic grazers as a function of concentration of food. *Limnology and Oceanography* 20, 259–262.
- Nicholson, J.K., Lindon, J.C., Holmes, E., 1999. ‘Metabonomics’: understanding the metabolic responses of living systems to pathophysiological stimuli via multivariate statistical analysis of biological NMR spectroscopic data. *Xenobiotica* 29, 1181–1189.
- Nisbet, R.M., Muller, E.B., Lika, K., Kooijman, S.A.L.M., 2000. From molecules to ecosystems through dynamic energy budget models. *Journal of Animal Ecology* 69, 913–926.
- O'Brien, W.J., Kettle, D., Riessen, H.P., 1979. Helmets and invisible armor: structures of reducing predation from tactile and visual planktivores. *Ecology* 60, 287–294.
- Okubo, A., Anderson, J.J., 1984. Models for zooplankton swarms: their formation and maintenance. *EOS* 65, 731–732.
- Parsons, T.R., LeBrasseur, R.J., Fulton, J.D., Kennedy, O.D., 1969. Production studies in the Strait of Georgia. Part II. Secondary production under the Fraser River plume, February to May, 1967. *Journal of Experimental Marine Biology and Ecology* 3, 39–50.
- Perhar, G., Arhonditsis, G.B., 2009. The effects of seston food quality on planktonic food web patterns. *Ecological Modelling* 220, 805–820.
- Perhar, G., Arhonditsis, G.B., Brett, M.T., 2012b. Modeling the role of highly unsaturated fatty acids in planktonic food web processes: a mechanistic approach. *Environmental Reviews* 20, 155–172.
- Perhar, G., Arhonditsis, G.B., Brett, M.T., 2012c. Modeling the role of highly unsaturated fatty acids in planktonic food web processes: sensitivity analysis and examination of contemporary hypotheses. *Ecological Informatics* 13, 77–98.
- Persson, J., Vrede, T., 2006. Polyunsaturated fatty acids in zooplankton: variation due to taxonomy and trophic position. *Freshwater Biology* 51, 887–900.
- Power, M., 1993. The predictive validation of ecological and environmental models. *Ecological Modelling* 68, 33–50.
- Ramin, M., Perhar, G., Shimoda, Y., Arhonditsis, G.B., 2012. Examination of the effects of nutrient regeneration mechanisms on plankton dynamics using aquatic biogeochemical modeling. *Ecological Modelling* 240, 139–155.
- Ravet, J.L., Brett, M.T., 2006. Phytoplankton essential fatty acid and phosphorus content constraints on *Daphnia* somatic growth and reproduction. *Limnology and Oceanography* 51, 2438–2452.
- Ravet, J.L., Brett, M.T., Arhonditsis, G.B., 2010. The effects of seston lipids on zooplankton fatty acid composition in Lake Washington. *Ecology* 91, 180–190.
- Rosenzweig, M., 1971. The paradox of enrichment. *Science* 171, 385–387.
- Roy, S., Chattopadhyay, J., 2007. The stability of ecosystems. A brief overview of the paradox of enrichment. *Journal of Bioscience* 32, 421–428.
- Royle, J.A., Dorazio, R.M., 2008. *Hierarchical Modeling and Inference in Ecology*. Academic Press.
- Seuront, L., Brewer, M.C., Strickler, J.R., 2003. Quantifying zooplankton swimming behaviour: the question of scale. *Handbook of Scaling Methods in Aquatic Ecology: Measurement, Analysis, Simulation*. CRC Press.
- Sherr, E.B., Sherr, B.F., Paffenhofer, G.A., 1986. Phagotrophic protozoa as food for metazoans: a missing trophic link in marine pelagic food webs? *Marine Microbial Food Webs* 1, 61–80.
- Sjoberg, S., 1980. Zooplankton feeding and queueing theory. *Ecological Modelling* 10, 215–225.
- Smyntek, P.M., Teece, M.A., Schulz, K.L., Storch, A.J., 2008. Taxonomic differences in the essential fatty acid composition of groups of freshwater zooplankton relate to reproductive demands and generation time. *Freshwater Biology* 53, 1768–1782.
- Strickler, J.R., 1998. Observing free-swimming copepods mating. *Philosophical Transactions of Royal Society of London B* 353, 671–680.
- Tiselius, P., 1992. Behavior of *Acartia tonsa* in patchy food environments. *Limnology and Oceanography* 37, 1640–1651.
- Tiselius, P., Jonsson, P.R., 1990. Foraging behaviour of six calanoid copepods: observations and hydrodynamic analysis. *Marine Ecology Progress Series* 66, 23–33.
- Tiselius, P., Jonsson, P.R., Karrtvedt, S., Olsen, E.M., Jordstad, T., 1997. Effects of copepod foraging behavior on predation risk: an experimental study of the predatory copepod *Pareuchaeta norvegica* feeding on *Acartia clausi* and *A. tonsa* (Copepoda). *Limnology and Oceanography* 42, 164–170.
- Titelman, J., 2001. Swimming and escape behavior of copepod nauplii: implications for predator–prey interactions among copepods. *Marine Ecology Progress Series* 213, 203–213.
- Van Donk, E., Hessen, D.O., 1993. Grazing resistance in nutrient-stressed phytoplankton. *Oecologia* 93, 508–511.
- vanDuren, L.A., Videler, J.J., 1995. Swimming behaviour of development stages of the calanoid copepod *Temora longicornis* at different food concentrations. *Marine Ecology Progress Series* 126, 153–161.
- vanDuren, L.A., Videler, J.J., 1996. The trade-off between feeding mate seeking and predator–prey avoidance in copepods: behavioural responses to chemical cues. *Journal of Plankton Research* 18, 805–818.
- Viant, M.R., 2007. Metabolomics of aquatic organisms: the new ‘omics’ on the block. *Marine Ecology Progress Series* 332, 301–306.
- Wainman, B.C., McQueen, D.J., Lean, R.S., 1993. Seasonal trends in zooplankton lipid concentration and class in freshwater lakes. *Journal of Plankton Research* 15, 1319–1332.
- Yen, J., Strickler, J.R., 1996. Advertisement and concealment in the plankton: what makes a copepod hydrodynamically conspicuous? *Invertebrate Biology* 115, 191–205.
- Zhao, J., Ramin, M., Cheng, V., Arhonditsis, G.B., 2008a. Competition patterns among phytoplankton functional groups: how useful are the complex mathematical models? *Acta Oecologica* 33, 324–344.
- Zhao, J.Y., Ramin, M., Cheng, V., Arhonditsis, G.B., 2008b. Plankton community patterns across a trophic gradient: The role of zooplankton functional groups. *Ecological Modelling* 213, 417–436.

**MODELING ZOOPLANKTON GROWTH IN  
LAKE WASHINGTON:  
A MECHANISTIC APPROACH TO PHYSIOLOGY  
IN A EUTROPHICATION MODEL.  
*ELECTRONIC SUPPLEMENTARY MATERIAL***

**Gurbir Perhar\*, George B. Arhonditsis**

Ecological Modeling Lab, University of Toronto,  
1265 Military Trail, Scarborough, Ontario, M1C-1A4, Canada

**Michael T. Brett**

Department of Civil & Environmental Engineering, University of Washington,  
Seattle, Washington, USA, 98195-2700

\*Corresponding author

E-mail: g.perhar@mail.utoronto.ca, Tel.: +1 416-287-7690; Fax: +1 416-287-7279.

# Description of the eutrophication model

**1. Nutrient cycles.** The organic carbon pool is modelled in both particulate and dissolved forms, and is fuelled by phytoplankton basal metabolism, zooplankton basal metabolism and zooplankton egestion of excess carbon during feeding (see Fig. 1). A fraction of particulate organic carbon (POC) undergoes a first order dissolution to form dissolved organic carbon (DOC), and an additional fraction of POC settles to the sediment. Zooplankton graze on POC via detritivory. First order reactions for denitrification and respiration during heterotrophic activity account for DOC losses.

Nitrogen compartments considered in the original model include nitrate, ammonium, dissolved organic nitrogen (DON) and particulate organic nitrogen (PON; see Fig. 1c). Phytoplankton incorporate ammonium and nitrate during growth, and the Wroblewski (1977) model is used to describe the inhibition of nitrate uptake by ammonium. The ammonium and DON pools are fuelled by phytoplankton basal metabolism and zooplankton basal metabolism. A fraction of PON hydrolyzes to DON, and an additional fraction settles to the sediment. A fraction of DON is mineralized to form ammonium, and ammonium oxidizes to nitrate through nitrification in the presence of oxygen. Nitrification kinetics are driven by ammonium availability, dissolved oxygen, temperature and light (Cercu and Cole, 1994; Tian et al., 2001). In anoxic conditions, nitrate is lost as nitrogen gas via denitrification.

Phosphorus compartments in the Lake Washington model include phosphate, dissolved organic phosphorus (DOP), and particulate organic phosphorus (POP; see Fig. 1d). Phytoplankton assimilates phosphate, and redistributes all three forms through basal metabolism; zooplankton basal metabolism and egestion also releases all three forms. Losses to the POP pool result from zooplankton grazing (detritivory), hydrolysis to DOP, and settling to the sediment. A first order reaction mineralizes DOP to phosphate, and additional phosphate gains and losses via external loading and outflows are considered.

Silica is modelled in dissolved and particulate forms. Diatoms uptake silica in dissolved

form, and recycle both dissolved and particulate. Particulate silica is subject to a first order dissolution to dissolved form and settling to the sediment. Dissolved oxygen sources and sinks include phytoplankton photosynthesis and respiration, zooplankton respiration, nitrification and atmospheric reaeration.

**2. Phytoplankton** Phytoplankton compartments consider biomass accrual through production, and losses through basal metabolism, settling, and herbivorous zooplankton grazing. Inorganic carbon is assumed to be in excess (Arhonditsis and Brett, 2005a). Phosphorus and nitrogen dynamics in cells account for luxury uptake, whereby uptake is driven by internal and external nutrient concentrations, but confined by upper and lower internal quota bounds (Hamilton and Schladow, 1997; Asaeda and Van Bon, 1997; Arhonditsis et al., 2002). The impacts of nutrients, light and temperature on phytoplankton growth are considered using a multiplicative model (Cerco and Cole, 1994). Light saturation curves and photosynthetic activity with depth are modelled following Jassby and Platt (1976) and Steele's equation with Beer's law, respectively. The extinction coefficient is taken as the sum of background light attenuation and attenuation due to chlorophyll-a. The dependence of phytoplankton growth on temperature is modelled as a Gaussian distribution. Basal metabolism accounts for the losses via respiration, excretion and natural mortality, increasing exponentially with temperature.

The three phytoplankton functional groups (diatoms, greens, cyanobacteria) are modelled to differ in their morphological features (settling velocities and shading effects), metabolic rates, and resource competition with regards to phosphorus, nitrogen, light and temperature. Diatoms are modelled as r-selected high quality algae. The traits associated with an r-strategist include high maximum growth rate and high metabolic losses. Additional traits include strong phosphorus kinetics, weak nitrogen kinetics, low tolerance to low light, low temperature optima, and high sinking velocity. Conversely, cyanobacteria are modelled as K-selected low quality algae. The traits associated with a K-strategist include low maximum growth rate and low metabolic rates. Additional traits include

weak phosphorus kinetics, strong nitrogen kinetics, high tolerance to low light availability, high temperature optima, low settling velocity and higher shading effects resultant of morphological features (e.g., filamentous cyanobacteria). Green algae are modelled as intermediate competitors between diatoms and cyanobacteria, and are present to more realistically depict the seasonal continuum between diatoms and cyanobacteria (Arhonditsis and Brett, 2005a).

**3. Zooplankton** In the original Lake Washington model, the two zooplankton functional groups are copepods and cladocerans, following general characteristics of *Diaptomus* and *Daphnia*-like species, respectively. Carnivorous zooplankton do not significantly impact these two groups of zooplankton in Lake Washington (Edmondson and Litt, 1982), and mortality resultant of omnivory is accounted for in the predation closure term. General characteristics for each grazer include: temperature limitation, food preference, selectivity strategy, stoichiometry and vulnerability to predators. These differences drive succession patterns and govern interactions with phytoplankton and particulate matter. Cladocerans are modelled as filter feeders and select food based on the respective abundance of the four food types (diatoms, green algae, cyanobacteria, detritus). Copepods are selective feeders, and selection is based on their ability to distinguish and ingest favourable food types at different concentrations. The cladoceran closure term is a sigmoidal curve, representing a switchable-type response, whereas the copepod closure term is a hyperbolic response, yielding higher predation rates at lower densities and the opposite when zooplankton are abundant.

<b>Diatoms</b>					
<b>JAN</b>	<b>FEB</b>	<b>MAR</b>	<b>APR</b>	<b>MAY</b>	<b>JUN</b>
(+)W <sub>loading</sub> *	(+)W <sub>loading</sub> *	(+)W <sub>loading</sub> *	(+)W <sub>loading</sub>	(+)N <sub>Ocope</sub> *	(-)DI <sub>EPA:C</sub>
(-)DI <sub>EPA:C</sub>	(-)DI <sub>DHA:C</sub>	(-)DI <sub>DHA:C</sub> *	(+)N <sub>Ocope</sub>	(+)P <sub>Mclad</sub>	(-)π <sub>MAXclad</sub>
(-)DI <sub>DHA:C</sub>	(-)DI <sub>EPA:C</sub>	(-)P <sub>Ocope</sub>	(-)DI <sub>DHA:C</sub>	(+)W <sub>loading</sub>	(+)P <sub>Oclad</sub>
(+)DHA <sub>Ocope</sub>	(-)P <sub>Ocope</sub>	(-)DI <sub>EPA:C</sub>	(+)P <sub>Mclad</sub>	(+)N <sub>Mcope</sub>	(+)W <sub>loading</sub>
(-)m <sub>cope</sub>	(+)DHA <sub>Ocope</sub>	(+)N <sub>Mcope</sub>	(+)N <sub>Mcope</sub>	(-)DI <sub>DHA:C</sub>	(-)ρ <sub>clad</sub>
<b>JUL</b>	<b>AUG</b>	<b>SEP</b>	<b>OCT</b>	<b>NOV</b>	<b>DEC</b>
(+)W <sub>loading</sub> *					
(-)DI <sub>EPA:C</sub> *	(+)P <sub>Mclad</sub>	(+)P <sub>Mclad</sub>	(-)DI <sub>EPA:C</sub>	(-)DI <sub>EPA:C</sub>	(-)DI <sub>EPA:C</sub>
(-)m <sub>cope</sub>	(-)m <sub>cope</sub>	(-)P <sub>Ocope</sub>	(-)m <sub>cope</sub>	(-)P <sub>Ocope</sub>	(-)P <sub>Ocope</sub>
(+)P <sub>Mclad</sub>	(-)P <sub>Ocope</sub>	(-)m <sub>cope</sub>	(-)P <sub>Ocope</sub>	(-)m <sub>cope</sub>	(-)m <sub>cope</sub>
(+)GR <sub>EPA:C</sub>	(+)DHA <sub>Ocope</sub>	(-)N <sub>Oclad</sub>	(+)ν <sub>clad</sub>	(+)GR <sub>EPA:C</sub>	(+)P <sub>Mclad</sub>

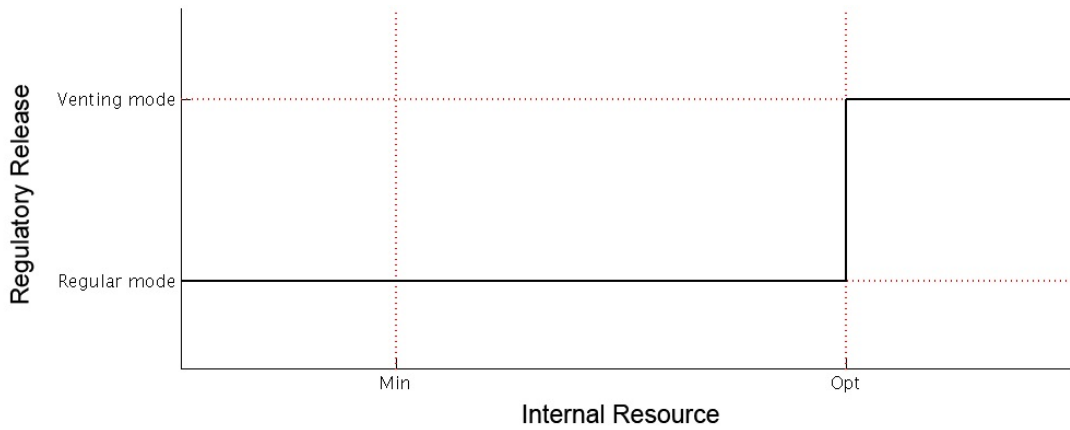
<b>Greens</b>					
<b>JAN</b>	<b>FEB</b>	<b>MAR</b>	<b>APR</b>	<b>MAY</b>	<b>JUN</b>
(+)W <sub>loading</sub> *	(-)DI <sub>EPA:C</sub>				
(+)DHA <sub>Ocope</sub>	(+)DHA <sub>Ocope</sub>	(+)DHA <sub>Ocope</sub>	(+)P <sub>Mclad</sub>	(+)P <sub>Mclad</sub>	(+)W <sub>loading</sub>
(+)GR <sub>EPA:C</sub>	(-)P <sub>Ocope</sub>	(-)P <sub>Ocope</sub>	(-)P <sub>Ocope</sub>	(-)P <sub>Ocope</sub>	(-)π <sub>MAXclad</sub>
(-)m <sub>cope</sub>	(+)P <sub>Mclad</sub>	(+)P <sub>Mclad</sub>	(+)DHA <sub>Ocope</sub>	(+)DHA <sub>Ocope</sub>	(+)P <sub>Oclad</sub>
(-)P <sub>Ocope</sub>	(-)m <sub>cope</sub>	(-)m <sub>cope</sub>	(-)DHA <sub>Mcope</sub>	(-)m <sub>cope</sub>	(-)m <sub>cope</sub>
<b>JUL</b>	<b>AUG</b>	<b>SEP</b>	<b>OCT</b>	<b>NOV</b>	<b>DEC</b>
(+)W <sub>loading</sub> *					
(-)DI <sub>EPA:C</sub>	(+)DHA <sub>Ocope</sub>	(+)GR <sub>EPA:C</sub>	(+)GR <sub>EPA:C</sub>	(+)GR <sub>EPA:C</sub>	(-)P <sub>Ocope</sub>
(-)m <sub>cope</sub>	(+)T <sub>Ncope</sub>	(-)m <sub>cope</sub>	(-)m <sub>cope</sub>	(-)P <sub>Ocope</sub>	(+)GR <sub>EPA:C</sub>
(+)GR <sub>EPA:C</sub>	(+)P <sub>Mclad</sub>	(-)P <sub>Ocope</sub>	(-)P <sub>Ocope</sub>	(-)m <sub>cope</sub>	(-)m <sub>cope</sub>
(+)P <sub>Mclad</sub>	(-)m <sub>cope</sub>	(+)P <sub>Mclad</sub>	(-)J <sub>PUFAcb</sub>	(+)DHA <sub>Ocope</sub>	(+)DHA <sub>Ocope</sub>

<b>Cyanobacteria</b>					
<b>JAN</b>	<b>FEB</b>	<b>MAR</b>	<b>APR</b>	<b>MAY</b>	<b>JUN</b>
(+)J <sub>PUFAcb</sub>	(-)m <sub>cope</sub>	(-)m <sub>cope</sub>	(+)W <sub>loading</sub>	(-)m <sub>cope</sub>	(+)J <sub>PUFAcb</sub>
(-)m <sub>cope</sub>	(+)J <sub>PUFAcb</sub>	(+)W <sub>loading</sub>	(-)m <sub>cope</sub>	(+)W <sub>loading</sub>	(-)m <sub>cope</sub>
(-)χ <sub>Nclad</sub>	(-)χ <sub>Nclad</sub>	(+)J <sub>PUFAcb</sub>	(+)EPA <sub>Oclad</sub>	(+)J <sub>PUFAcb</sub>	(-)χ <sub>Nclad</sub>
(+)EPA <sub>Oclad</sub>	(+)EPA <sub>Oclad</sub>	(-)χ <sub>Nclad</sub>	(-)χ <sub>Nclad</sub>	(+)EPA <sub>Oclad</sub>	(+)EPA <sub>Oclad</sub>
(+)ρ <sub>clad</sub>	(+)ρ <sub>clad</sub>	(+)EPA <sub>Oclad</sub>	(+)J <sub>PUFAcb</sub>	(-)χ <sub>Nclad</sub>	(-)h <sub>DHAclad</sub>
<b>JUL</b>	<b>AUG</b>	<b>SEP</b>	<b>OCT</b>	<b>NOV</b>	<b>DEC</b>
(-)χ <sub>Nclad</sub>	(-)χ <sub>Nclad</sub>	(-)χ <sub>Nclad</sub>	(-)χ <sub>Nclad</sub>	(+)W <sub>loading</sub>	(+)W <sub>loading</sub>
(+)EPA <sub>Oclad</sub>	(+)J <sub>PUFAcb</sub>	(+)ρ <sub>clad</sub>	(+)W <sub>loading</sub>	(-)χ <sub>Nclad</sub>	(+)DHA <sub>Ocope</sub>
(+)J <sub>PUFAcb</sub>	(+)ρ <sub>clad</sub>	(-)T <sub>Nclad</sub>	(-)T <sub>Nclad</sub>	(-)T <sub>Nclad</sub>	(-)χ <sub>Nclad</sub>

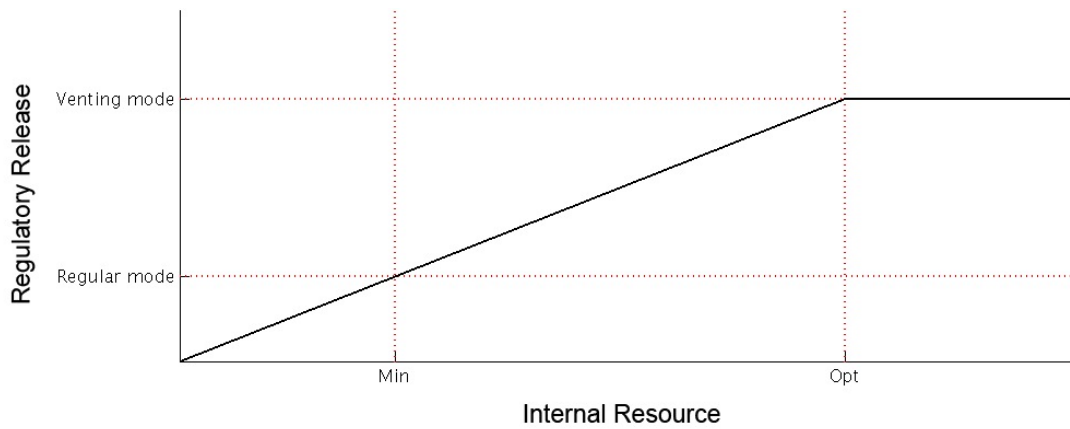
(-) $m_{cope}$	(+) $\rho_{cope}$	(+) $\rho_{cope}$	(+) $\rho_{clad}$	(+) $\chi_{Ncope}$	(-) $T_{Nclad}$
(-) $h_{DHAclad}$	(-) $W_{EPItemp}$	(+) $\chi_{Ncope}$	(+) $\chi_{Ncope}$	(+) $DHA_{Ocope}$	(+) $\chi_{Ncope}$

---

Table 1: Multiple regression analysis of the most influential model parameters for phytoplankton biomass listed by month at present conditions.



(a) Present strategy alternating between regular mode and *venting* mode using threshold dynamics



(b) Alternate strategy employing Holling type II response to continually adjust excretion in response to physiological conditions until a threshold is passed at which point *venting* mode is activated

Figure 1: Somatic regulatory response curves.

# 1 Bibliography

## References

- Arhonditsis, G.B., Brett, M.T., 2005a. Eutrophication model for Lake Washington (USA) Part I. Model description and sensitivity analysis. *Ecol Model* 187, 140–78.
- Arhonditsis, G.B., Tsirtsis, G., Karydis, M., 2002. The effects of episodic rainfall events to the dynamics of coastal marine ecosystems: applications to a semi-enclosed gulf in the Mediterranean Sea. *J Mar Syst* 35, 183–205.
- Asaeda, T., Van Bon, T., 1997. Modelling the effects of macrophytes on algal blooming in eutrophic shallow lakes. *Ecol Model* 104, 261–87.
- Cerco, C.F., Cole, T.M., 1994. CE-QUAL-ICM: a three-dimensional eutrophication model, version 1.0. User's Guide. US Army Corps of Engineers Waterways Experiments Station, Vicksburgh, MS.
- Edmondson, W.T., Litt, A.H., 1982. Daphnia in Lake Washington. *Limnol Oceanogr* 27, 272–93.
- Hamilton, D.P., Schladow, S.G., 1997. Prediction of water quality in lakes and reservoirs. Part 1. Model description. *Ecol Model* 96, 91–110.
- Jassby, A.D., Platt, T., 1976. Mathematical formulation of relationship between photosynthesis and light for phytoplankton. *Limnol Oceanogr* 21, 540–547.
- Tian, R.C., Vezina, A.F., Starr, M., Saucier, F., 2001. Seasonal dynamics of coastal ecosystems and export production at high latitudes: a modeling study. *Limnol Oceanogr* 46, 1845–59.
- Wroblewski, J.S., 1977. Model of phytoplankton plume formation during variable Oregon upwelling. *J Mar Res.* 35, 357–94.